Tailoring the Gr/Si heterointerface by decorating CdSe/ZnS QDs for Photovoltaics

By

Mazhar Tanveer Afzal Naz

School of chemical and Materials Engineering

National University of Sciences and Technology

2021

Tailoring the Gr/Si heterointerface by decorating CdSe/ZnS QDs for Photovoltaics

Mazhar Tanveer Afzal Naz

Reg.No:00000277676

This thesis is submitted as a partial fulfillment of the requirements for the degree of

MS in Nano Science and Engineering

Supervisor Name: Dr. Muhammad Shoaib Butt

School of Chemical and Materials Engineering (SCME)

National University of Sciences and Technology (NUST)

H-12 Islamabad, Pakistan

August 2021

DEDICATION

I dedicate this thesis to, my beloved Parents who have been a constant source of inspiration, my brother and my sister for their love and support, and my future wife.

Acknowledgment

All gratitude and praises are to **Allah Almighty**, the Most Gracious and the Most Merciful. He is the entire source of knowledge and wisdom to mankind, who gave us health, thoughts, and capacitated us to achieve this goal. After Almighty Allah, praises are to His **Prophet Muhammad (S. A.W.),** the most Perfect and Exalted, and an everlasting source of Guidance and Knowledge for humanity as a whole.

I would like to express my deepest and sincere gratitude to my supervisor **Dr. Muhammad Shoaib Butt** and Co-supervisor **Prof. Dr. Arshad Saleem Bhatti**, Rector Virtual University who accepted me as a postgraduate student and provided me a chance to work with them. I am truly very fortunate to have the opportunity to work under their supervision and grateful for my advisement, guidance, and support throughout my work. The professional research skill and personal lessons that I have learned from them are invaluable for future endeavors. Also, I am very grateful to all my teachers who helped me and motivated me to do my best.

I am greatly indebted to all my colleagues in CMND, COMSATS who have graciously applied themselves to the task of helping me with support and valuable suggestions. A special thanks to **Dr. Fahad Bhopal** and all the other senior research students for their help and support. I pay my regards to my colleagues and friends especially Muhammad Hasan, Rizwan Zafar, And Muhammad Bilal, thanks for the friendship and memories.

Finally, I am thankful to my family, especially my parents and siblings. Their moral help and financial support remained with me throughout these years.

-Mazhar Tanveer Afzal Naz

Abstract

Photovoltaic devices are an emerging technology in this study, we fabricated a large area and reliable Graphene/Silicon solar cell by introducing Quantum Dots for 540nm and 650nm wavelength emission. Silicon Dioxide was grown by thermal oxidation. Gr/Si heterojunction was made by use of lithography. Graphene was grown by CVD and then transferred to Si to make the heterojunction. Quantum dots were coated by drop-casting and characterization was done for electrical properties. Monolayer graphene was confirmed by Raman spectroscopy. And I_D band shows that the graphene was very less defective. Emission spectra of QD's were confirmed by Photoluminescence with bands at 527nm and 650 nm. Electrical properties were studied by Current-voltage and capacitance-voltage characterization. A clear enhance in current density and efficiency has been noted. Around 134% increase in current density is being observed with about 265% increase in Efficiency. Results show that Quantum Dots of CdSe/ZnS has good optical properties when it interacts with Graphene/Silicon solar cell structure and helps improve Photo Conversion Efficiency. This shows a promising future of quantum dots as the top layer of solar cells.

Table of Contents

List of Figures

List Of Tabels

Chapter 1

Introduction and Literature Review

1.1 NANOTECHNOLOGY

Humans have made major technological advancements in the past three or four decades. All the new inventions have been making life easy, but everything needs fuel to work. As the natural resources on earth are not everlasting so they will end in the coming decades. In the wake of this crisis, humans need a renewable energy source that can work as efficiently as natural resources. The most widely explored alternative is the solar cell in which sunlight is used as fuel to generate electricity.

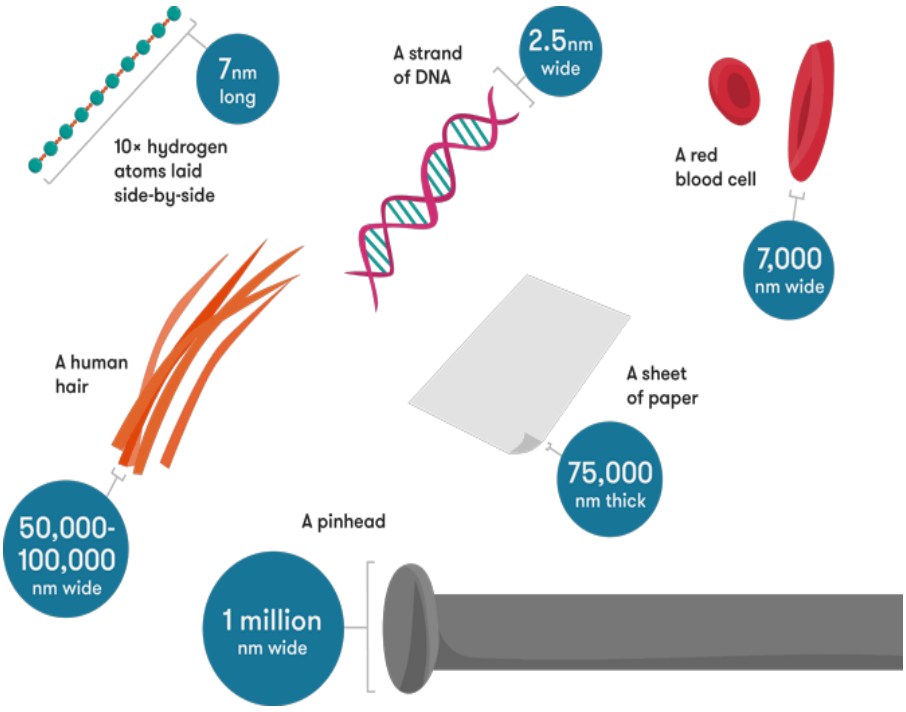

Figure 1.1: Nanoscience with scale

1.1.1 Applications of Nanoscience and Nanotechnology

Nanotechnology is an exceptionally wide field that includes surface science, natural chemistry, atomic science, and semiconductor physics, modeling, and controlling matter at the nanoscale [1]. Nanotechnology is capable of producing numerous modern types of equipment and gadgets with tremendous applications in pharmaceutical, biotechnology, and energy storage.

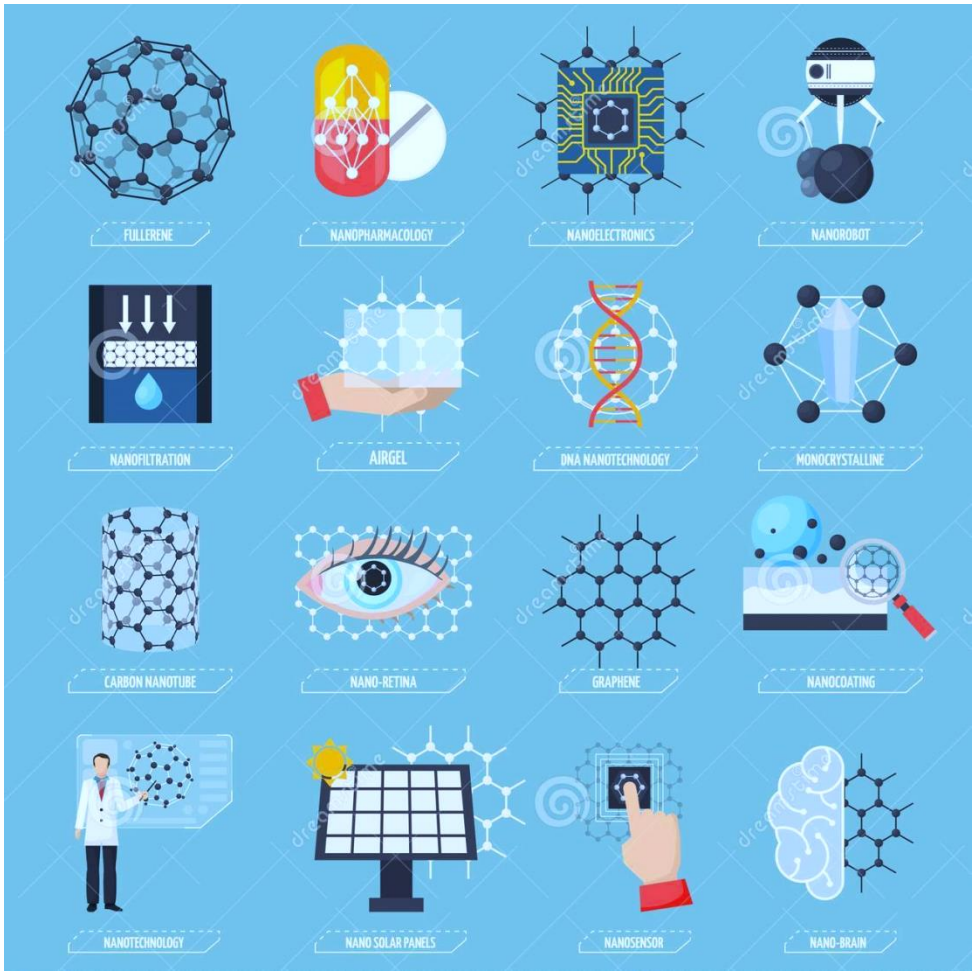

Figure 1.2: Applications of Nanotechnology[2]

1.1.2 Dimensional Classification of Materials

Materials can be classified dimensionally based on nanostructure elements present in that material having dimensions as three, two, one, and zero. The dimensional classification shows the degrees of freedom in particle momentum. The relation between the density of states and the energy of materials in different dimensions is shown in Figure 1.3. The density of state changes significantly as we move from bulk to zero-dimensional material as the degree of confinement also varies with a dimension of material. Examples of nanostructures in different dimensions are demonstrated in the Figure below.

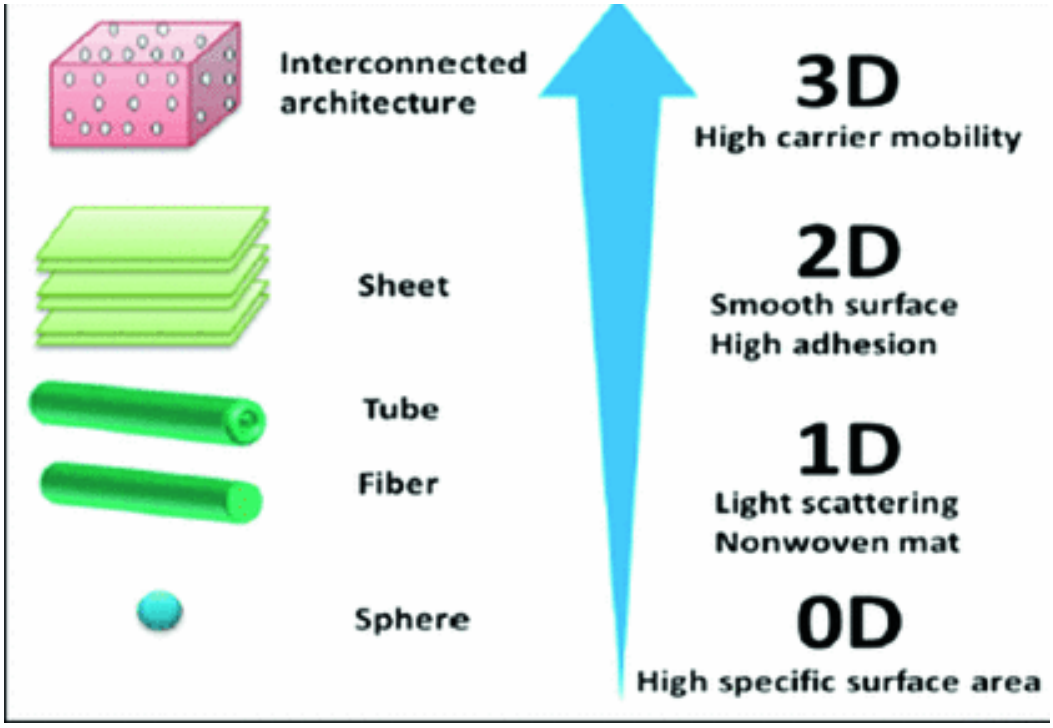

Figure 1.3: Classification of Nanomaterials [3]

1.1.2.1 Zero Dimension

In zero-D, the motion of electrons is confined in every direction. Examples are quantum dots, nanoclusters, etc.

1.1.2.2 One Dimension

In 1-D, electrons can move freely in a single direction; the motion is restrained in the remaining two directions. Examples are nanorods and nanowires etc.

1.1.2.3 Two Dimension

In 2-D, electrons can move freely in two directions; the motion is restrained in a single direction. Examples are branched structures and nanofilms etc.

1.1.2.4 Three Dimension

In 3-D, electrons can move freely in all possible directions. Examples are powders, polycrystalline materials, etc.

One of the many energy conversion alternatives used all around the globe, The most emphasis has been paid to solar cells (photovoltaic cells). Solar photovoltaics offer the ability to gather clean, renewable energy from the sun. The most difficult aspect of photovoltaic energy conversion is obtaining a considerable improvement in power conversion efficiency as shown in Figure 1.4.

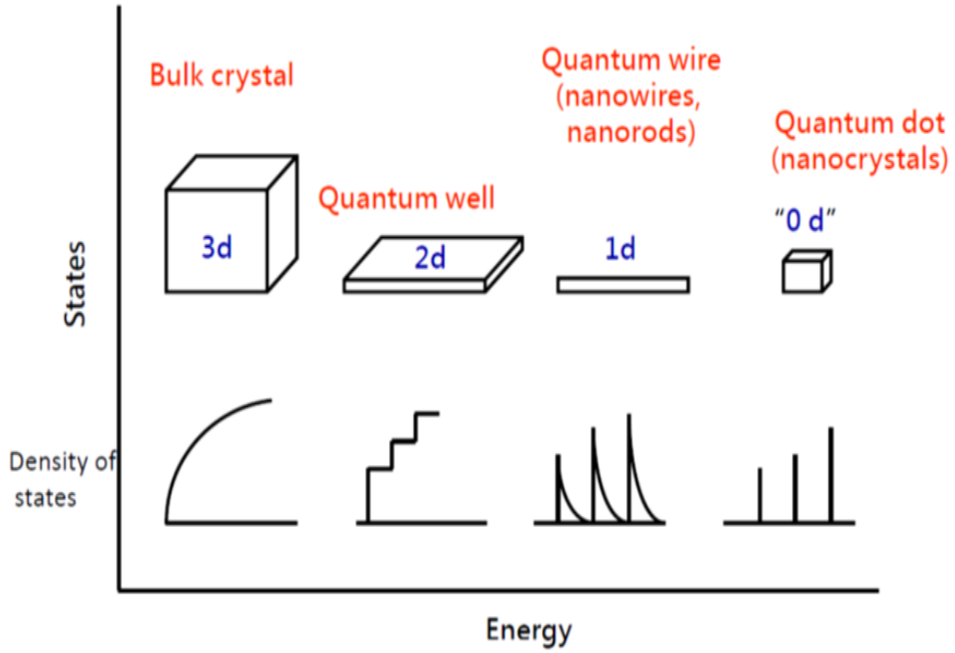

Figure 1.4:Zero dimensional, One dimensional, Two-dimensional, Three-dimensional materials and their density of states[4]

Due to silicon's availability on the globe and greater efficiency and stability than alternative energy sources, traditional wafer-based silicon solar cells continue to dominate the commercial solar cell market. [5,6]. Higher efficiency in the production of wafer-based solar cells, but on the other hand, has resulted in higher production costs. [7]. As a result, throughout the last few decades, various materials and innovative production technologies for solar cell development have garnered increased attention [8]. Hybrid and 2D materials-based solar cells have attracted a lot of attention due to their manufacturing at room temperature and variation in band structures. [9]. However, device stability remains a problem. and it is the principal impediment to their larger practical use [10].

1.2 SOLAR CELL

Photovoltaic (PV) devices may be roughly separated into three generations since the discovery of the photovoltaic effect, depending mostly on the timeliness of their introduction as shown in Figure 1.5. The first-generation solar cells were developed for the satellite application, these are single-junction devices fabricated with silicon wafers having an efficiency of 25%, while the maximum efficiency, as predicted by the Shockley–Queisser limit [11], is about 30%. Because this generation of PV technology has significant material and processing costs., the second generation of Photovoltaic systems was developed. For second-generation, efficiency up to 19% has been observed. As these second-generation solar cells have low material and processing costs as compared to first-generation solar cells but their reduced efficiency and difficulty of manufacturing wide-area solar cells has been a limiting issue. The most common materials used in this generation are Cadmium sulfide, Copper indium gallium selenide, and Cadmium Telluride. A low-cost future was expected to shape up with the introduction of revolutionary materials and device concepts from organic solar cells and Dye-Sensitized solar cells (DSSC)[12].

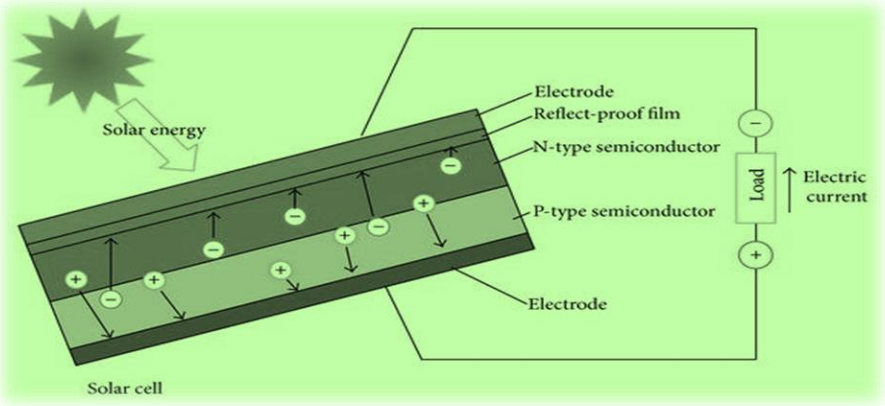

Figure 1.5: Solar Cell Schematic

The use of flexible substrates in demonstrations opened up new possibilities, and the building integrated design approach ushered in a new era in the renewable energy environment. [13]. For DSSCs, this approach has been carefully investigated for over a decade and has a maximum efficiency of 12%. This generation of devices has been hindered in its commercialization due to their reduced efficiency and stability.

1.3 COST

Using 0.2% of the incoming sun's radiation is adequate to fulfill our current energy needs. The expense of these technologies is a barrier to achieving this aim. Coal-fired power plants are the cheapest source of electricity, costing $0.04/kilowatt-hour (kWh), whereas PV costs $0.20 to $0.35 for the same amount of electricity. The processes involved in the creation of a PV module include the fabrication of a semiconductor absorber, the fabrication of PV cells, the assembling of PV modules, and the installation of the module. The final stage incorporates the cost of inverters and energy storage devices. PV modules account for 30-50 percent of the overall cost outlay, with linked expenses being greater for off-grid systems due to greater prices connected with storage devices [14]. According to the US government's Sunshot Initiative, PV modules cost around $0.5/W for a whole PV system costing $1/W [15] as shown in Figure 1.6. Thin-film technologies utilize less energy and have thinner semiconductor layers than traditional technologies, therefore, they are less expensive than Si modules. A CdTe module with a 17.5 percent efficiency now costs $0.61 per watt, but this is anticipated to drop to $0.35 per watt by 2017. [16]. The cost of a CIGS module with a 15.7 percent efficiency is projected to be $0.64/W. The crystalline technology, which is the most developed, dominates the PV industry. C-Si has an estimated market share of 85-90 percent, with thin-film technologies accounting for around 13 percent. The crystalline technology, which is the most developed, dominates the PV industry. C-Si has an estimated market share of 85-90 percent, with thin-film technologies

accounting for around 13 percent. Although significant cost reductions have been achieved over time, problems like resource scarcity and processing costs continue to obstruct the actual potential of these technologies. To generate solar grade material from metallurgical grade Si, processing a c-Si needs energy-intensive methods. At 500-600 oC5, CIGS and CdTe must be processed at high temperatures and under a high vacuum. Modules made of gallium arsenide (GaAs) are highly costly because they need epitaxial development.

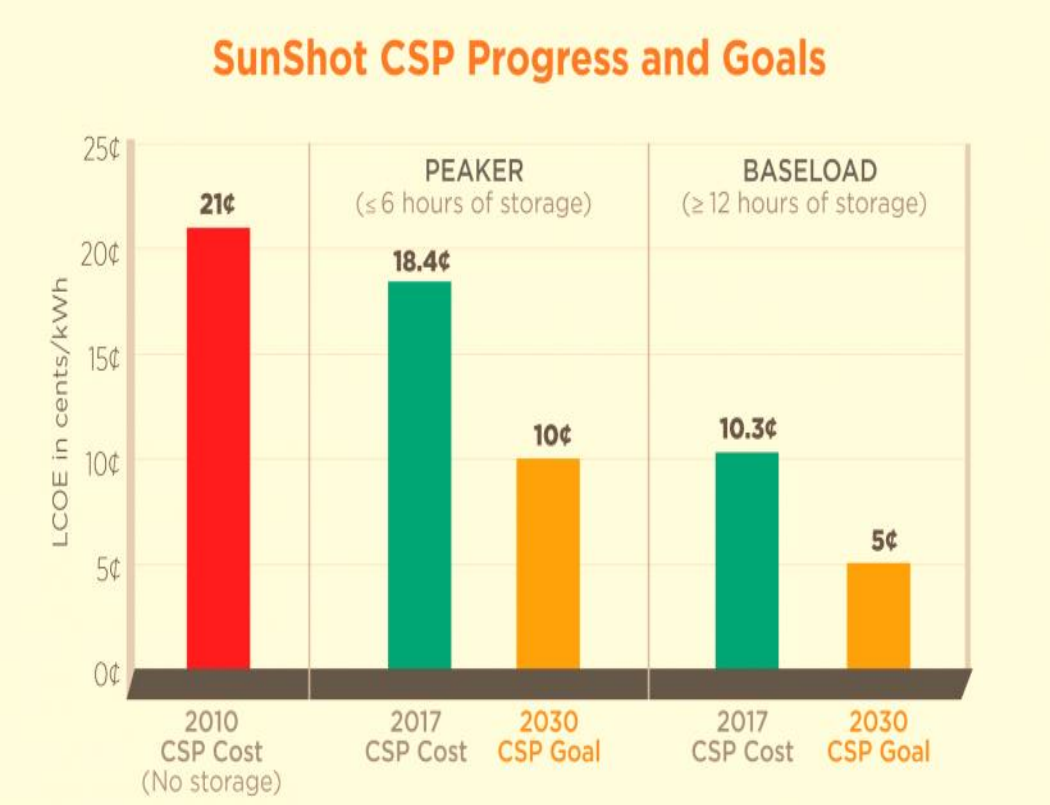

Figure 1.6: Sunshot Estimated Cost

5TW of PV module installed capacity is required to provide 16 percent of global power consumption by 2050. c-Si is the costliest of the existing technologies, and at 0.3TW, Te will be depleted. At 0.09 TW of installed capacity for CIGS, indium, gallium, and selenium are expected to be depleted. Methods based on abundant earth minerals and low-cost

technologies must be developed to meet the projected demand. Low-cost, low toxicity, abundant, and consistent material supply, scalable processing at low temperatures in ambient air, compatibility with a wide range of inexpensive substrates, acceptable efficiency, and stability are just a few characteristics for PV production. The material science community faces a tough challenge in selecting a suitable material since these properties are usually at variance with one another is shown in Figure 1.7. [17]. The 2-D materials-based solar cell is a recent development in PV technology. PV technology has shown a lot of promise for the future of solar cells as they have huge advantages in case of efficiency and cost-effectiveness. Earth-abundant materials are being used which make these devices low cost, also the solution processing for these photovoltaic devices can be done at low temperature which also is an advantage in regards to cost and time, other than that they have long diffusion lengths and high extinction coefficient which make them more efficient.

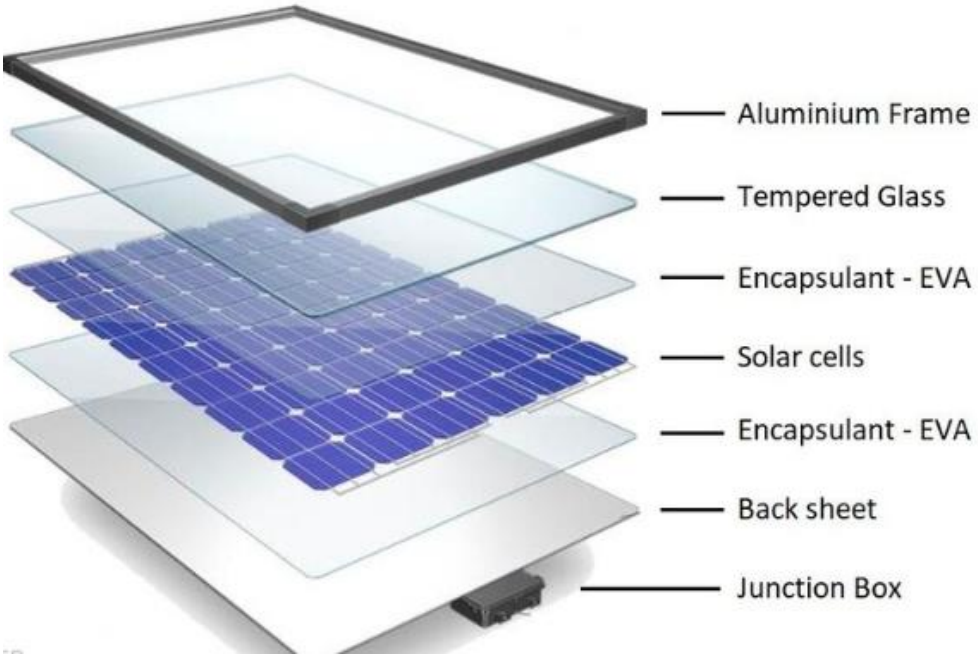

Figure 1.7: Solar Cell Construction[18]

They are also compatible with flexible substrates. But due to the use of Lead toxicity and long-term stability are still a concern as the international community is raising a loss of concern about the usage of lead because of its toxicity. Perovskites are calcium titanate-based materials with the ABX3 crystal structure. ABX3 is a structure that has already shown a lot of interesting properties such as superconduction, piezoelectricity, thermoelectricity, and anti-ferromagnetic behavior. Mostly, perovskites are be produced by solid-state mixing of precursor with the temperature over 1300°C. They may also be produced by drying a precursor salt solution, and those having semiconductor properties are particularly valuable in printed electronics due to their solution processabilityABX3 is the formula that describes the crystal structure of perovskites. A B and X have different sizes with A being larger than X, X is anion while A and B are cations. Crystallographic stability and its structure are being governed by tolerance factor t and an octahedral factor defined as the ratio of bond length.

The values of t between 0.89 and 1 dictate the cubic structure of perovskites, it also stabilizes the orthorhombic structure and less symmetric tetragonal structures. In most organic-inorganic halide perovskites methylammonium (CH3NH3) having rA value equals to 0.18 nm is being used, good findings for ethyl ammonium (CH3CH2NH3+) (rA = 0.23 nm) have also been published, (NH2 CH=NH2+) and amidine (NH2 CH=NH2+) Iodine (rX = 0.220 nm) is the most common anion X, although Br with rX = 0.196 nm and Cl with rX value 0.181 nm, are increasingly being reported in mixed halide configurations. Because of their smaller and theoretically perfect band gaps, for the sole reason of good efficiency, the Pb and Sn are being utilized as B cations in perovskite materials. The lower stability of Sn is owing to the ease with which it may be oxidized to SnI4, Relativistic effects, on the other hand, give higher oxidation protection in Pb. Thus, methylammonium lead triiodide (CH3NH3PbI3) is the typical compound,

with mixed halides CH3NH3PbI3xClx and CH3NH3PbI3xBrx also being significant.

1.4 PEROVSKITE-SENSITIZED SOLAR CELLS

The invention of the perovskite solar cell owns its origin in the DSSCs. Mesoporous titania which is an n-type material is sensitized with a light absorption Dye in a redox electrolyte. However, for the complete absorption of the dye's absorption spectrum larger sheet was required such as 10m, porous titania provides the sensitized dye with a larger interior surface area for effective absorption of incident photons. For solid-state DSSCs, the need for a 10 m thick active layer is unrealistic since the active layer thickness is limited to less than 2 m for several reasons. Which are allowing a complete light absorption spectrum and also boosting the amount of light absorbed into the Near-infrared region. Between 2006 and 2008, T. Miyasaka and for achieving more efficient DSSCs first perovskites solar cell was reported which used iodide Triiodide and a polypyrene carbon black composite with hole conductor. CH3NH3PbI3 and CH3NH3PbBr3 absorbers were used. The efficiencies of 0.4 and 2% were recorded for solid-state and liquid electrolyte cells for full-sun power. The full-sun power conversion efficiency of solid-state and liquid electrolyte cells was evaluated at 0.4 and 2%, respectively. In 2009, the very first study on perovskite-sensitized sola cell was published, which showed an efficiency of 3.5%, they used CH3NH3PbI3 as an absorber in the I/I_3 redox pair.

In figure 1.8 the design of a perovskite solar cell is shown. N.G.Park and coworkers[19] obtained 6.5 percent increased efficiency by using liquid electrolyte, while they also improved titania surface morphology and processing. However, use of liquid electrolyte caused the breakdown and disintegration of perovskites, as a result, the solar cells were unstable and would deteriorate within minutes. which became a hurdle in the pursuing of liquid electrolyte-based perovskite solar cells.

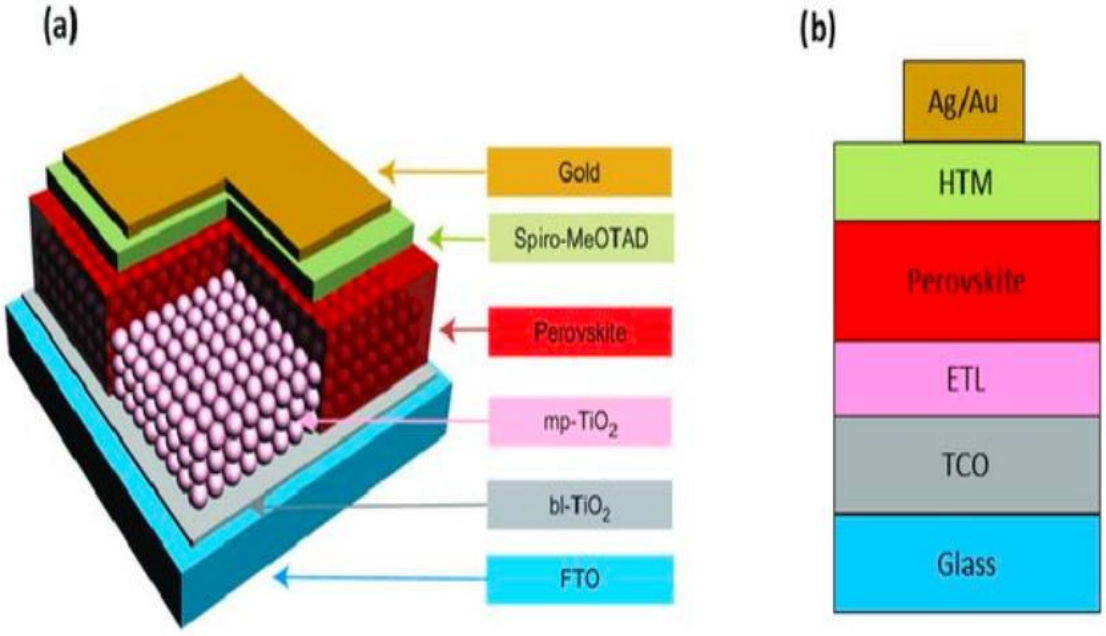

Figure 1.8: Schematic illustration of the (a) mesoscopic and (b) planar perovskite solar-cell configurations.

In 2008, Miyasaka and co-workers [20] tested the solid-state hole transport layer as an electrolyte which provided the solution for the breakdown of perovskites. Adoption of a solid-state hole transport medium in place of an electrolyte, as they made some other improvements in the structure of perovskites which enabled them to achieve efficiency up to 10% using mixed halide perovskites. This 10% efficiency was a clear improvement over the DSSCs, which gave the perovskite solar cells an edge over the DSSCs due to their full spectrum absorption for very thin layers such as 500nm. This proved as a significant improvement and paved way for further research in perovskite materials.

1.5 PLANAR HETEROJUNCTION STRUCTURED CELLS

The PCE of 15.4 percent 51 was achieved by thermally co-evaporating CH3N0H3I and PbCl2 and depositing CH3NH3PbI3xCl3 over FTO with a thin TiO2 layer. This demonstrates perovskites' dual role of photoexcitation and charge transfer. As a result, a mesoporous oxide layer may not be necessary. Due to better morphological control and the creation of a uniformly flat, pinhole-free active layer, the vapor-deposited perovskite layer has a higher PCE than the solution-treated active layer. While solution processing makes it simpler to get a flat CH3NH3PbI3xClx active layer, as it is challenging to get a homogenous CH3NH3PbI3 active layer. The combination of P3HT and PCBM has been widely studied in organic photovoltaics. In planer heterojunction solar cells CH3NH3PbI3 was used as a replacement for the photoactive layer, resulting in a higher PCE of 3.9 percent. PEDOT: Perovskite active layers coated with -butyrolactone solution exhibited greater wettability than PSS-coated ITO substrates with DMF solution. When the C60 self-assembled monolayer was applied to the ITO substrate, in terms of photovoltaic performance, a device structure based on TiO2/ CH3NH3PbI3xClx/P3HT performed better. PCE rose from 3.8 to 6.7 percent after a self-assembled monolayer was added. This was accomplished by significantly increasing Jsc and Voc. Hybrid planer heterojunction s are also reported and investigated, in which the layer of 285nm thickness was used which helped in obtaining PCE of 12%. The charge collecting surfaces were modified with chlorobenzene spin coating, while vacuum-deposited active layer using reagents CH3NH3I was heated to 70°C and PbI2 was heated 250°C.

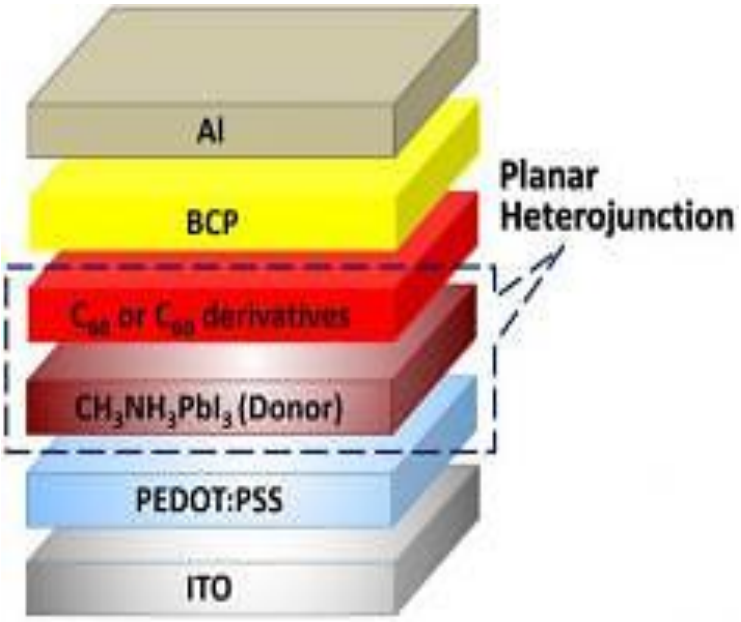

Figure 1.9: Planar Heterojunction Perovskites [21]

1.6 HYBRID MULTIJUNCTION SOLAR CELLS

In tandem solar cells the perovskites solar cells have tendency to be used as a top cell, in the second and third generation of solar cells, with a current density of 20 mA/cm2 and a top perovskite solar cell with Voc 1.1V, a silicon cell with a Voc of 0.75V will have an FF of 0.8 and an efficiency of 29.6% as shown in Figure 1.10. With just modest enhancements in bandgap widening, FF enhancement, and tandem cell design integration, all of this is possible with present technology.

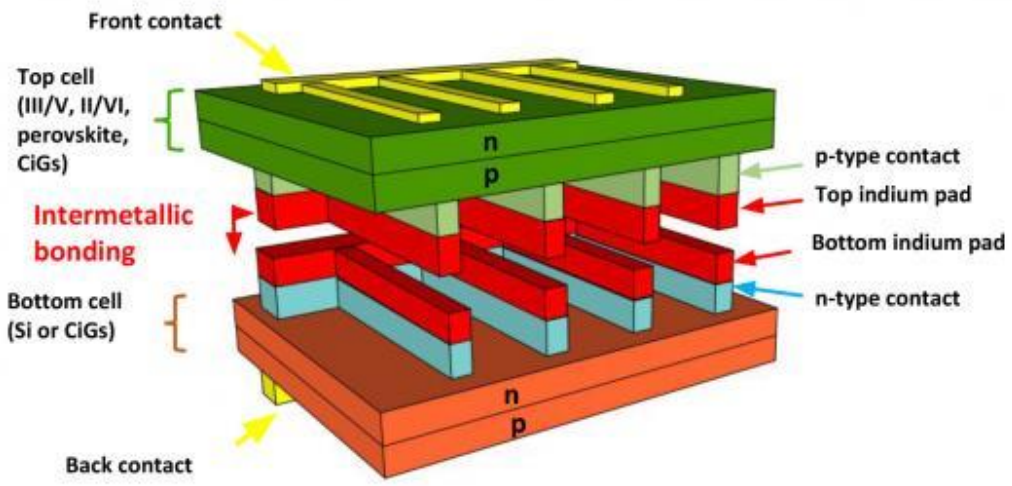

Figure 1.10: Multijunction Solar cell[22]

1.7 MATERIAL

Graphene is a two-dimensional substance that is an allotropic kind of carbon with atoms organized in a honeycomb lattice. The isolation approach is responsible for success. The proposed approach allowed the 2-D material to be isolated on the top of a 300-nm-thick silicon oxide chip. Adhesion between graphene and wafer is caused by weak van der Waals forces, and once on top of the wafer, the 2d material may be moved about, such as moving it from one substrate to another or suspending it over a trench, supported from one side. To form a three-dimensional material layer so graphene stacked up by using weak van der Waals forces. The strategy's creativity was to figure out a method to remove monolayer of graphene off graphite. 2.3 percent of white-light is being absorbed by monolayer graphene (97.7% transmittance), where is the fine-structure constant. The relationship between optical transparency, sheet resistance, and graphene layers is becoming more complex as the count of graphene layers increase, and therefore the range of layers may be described as a proportionate reduction

in both transparency and electrical sheet resistance. Single sheet of graphene has very high optical transparency up to 97.7 percent. whereas optical transparency of 3 layers of graphene is 90.8 percent, therefore, the optical transparency of each layer is reduced by 0.3 percent. A single sheet of graphene increases sheet resistance by twofold. It is a mono- layer of a carbon atom with special characteristics in photovoltaic applications, measuring 1 ksq^{-1} and 350 sq^{-1}.

Most of the work on 3rd generation solar cells is done in labs which is not commercially available due to their lack of meeting industrial requirements. MoS2 is a 2D material made up of single layer of atoms that was developed in the early twentieth century. Due to the distinct properties of Transitional metal dichalcogenides (TMDCs) have attracted lot of attention as their Physical , optical, and Photovoltaic properties are well established as compared to their bulk parents. Semiconducting MoS2 is an important 2D materials, overcoming graphene's zero band gap and allowing it to be used in new electrical and optoelectronic devices.

1.8 GRAPHENE

Graphene has emerged as a viable option for solar cell applications. Scientists all around the world are trying to enhance efficiency of solar cells by using different techniques. Quantum dots has shown lot of promising applications which can help in the enhancement of solar cell efficiency. As graphene is now well-known semi-conductor material which is used in different types of solar cells. Graphene/ silicon heterojunction which also known as Schottky junction was first time fabricated in 2010, having an efficiency of 1.65%.

In the photovoltaic industry, Schottky junction solar cells, are gaining a lot of prominence, they are made by directly depositing a thin layer of metal on top the transparent electrode. These are cheap and have very simple

manufacturing process. This makes them cheap as compared to conventional p-n junction solar cells.

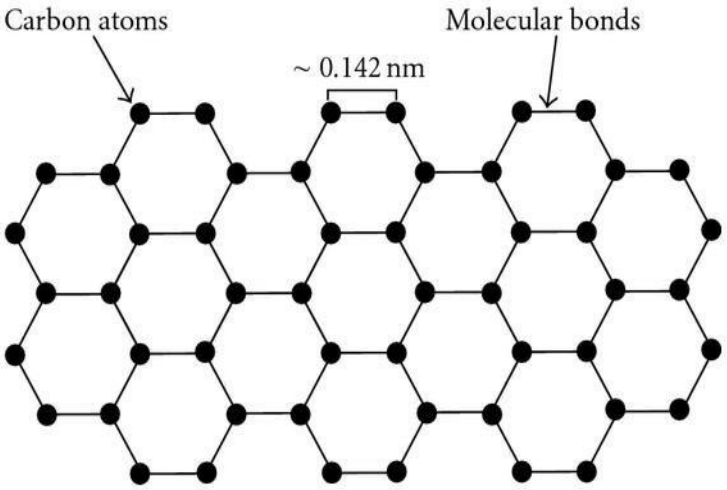

Figure 1.11: Structure of Graphene [23]

The metal layer was replaced with indium tin oxide (ITO) by the researchers. However, because to the scarcity of indium, production costs will be expensive, ITO's brittle nature will limit its use in flexible electronics. Geim and Novoselov were the first to manufacture graphene, a two-dimensional material model, through mechanical exfoliation from graphite in 2004. Because “it is made up of a single layer of carbon atoms packed together in a hexagonal form, it is a promising material with numerous unique properties”. Due to it superb optical characteristics graphene can efficiently avoid photon loss, with transparency reaching 97.7 percent in the NIR and in visible light.

Table 1.1: Properties of Graphene [24]

Charge carrier mobility	~200 000 $cm^2/V \cdot s$
Thermal conductivity	~5000 W/m·K
Transparency	~97.4%
Specific surface area	~2630 m^2/g
Young's modulus	~1 TPa
Tensile strength	~1100 GPa
Band gap	Zero

Carrier mobility of graphene approaches 104 $cm^2v^{-1}s^{-1}$ at ambient temperature, and its outstanding optical and electrical properties make it a feasible electrode in sensors, light emitting diodes and solar cells. Furthermore, because graphene is not only flexible but also plentiful on the planet, it has sparked great attention as low-cost electronics as an alternative for indium tin oxide (ITO) and fluorine tin oxide (FTO). Graphene may be utilised as n-type or p-type electrodes because of its adjustable work function. Properties of Graphene are written in Table 1.1. Considering graphene's remarkable optical and electrical properties, Zhu et al in 2010 reported the first Graphene/ silicon Schottky junction solar cell. Since then, there has been lot of work dine on the Gr/Si heterojunction. They demonstrated that graphene sheet, when coupled with Si, may be used to create effective solar cells. Graphene works as a transparency electrode in these solar cells, but it also plays a significant function in photo-carrier separation and transport.

1.9 QUANTUM DOTS

These small crystals known as Quantum dots have the ability to transport an electron, and they are made by people. Semiconducting nanoparticles produce a rainbow of shades when exposed to UV light It has benefitted composite materials, solar cells, and fluorescent biological markers by utilizing these semiconductor nanoparticles. Quantum dots are man-made nanostructures that, depending on their substance and form, can have a wide range of characteristics. The electrical properties of these materials make them ideal for use in single-electron transistors.

Figure 1.12: PL Quantum Dots[25]

In addition to its size, a QD's properties are determined by its shape, composition, and structure (such as whether it is solid or hollow), among other factors. An effective method of generating nanocrystals with the exact same characteristics every time must be able to produce vast numbers of nanocrystals with the same parameters every time. QDs have several uses in

catalysis, electronics, microelectronics, information storage, sensing, and medicine. All of these applications benefit from the small particle size and adjustable pore energy levels of QDs, including composites, solar cells (Grätzel cells)[26], and luminous biomedical markers.

1.10 GRAPHENE/SI SOLAR CELLS

Graphene Silicon heterojunction is shown in the figure below. The SiO2 layer is wet etched off a Si wafer using buffered HF solution to reveal a square window that defines the solar cell's active region. Photolithography and metal deposition are used to produce the front contact, as well as a conventional coating with n-Si on the front contact and single layer, bilayer, or multilayer graphene directly deposited onto the top of patterned substrates with the solution approach. Due to the mismatch of work function of the two materials, Graphene and n-type semiconductors A built-in electric field is generated when Si adjust their Fermi level to the common position in such devices. [27].

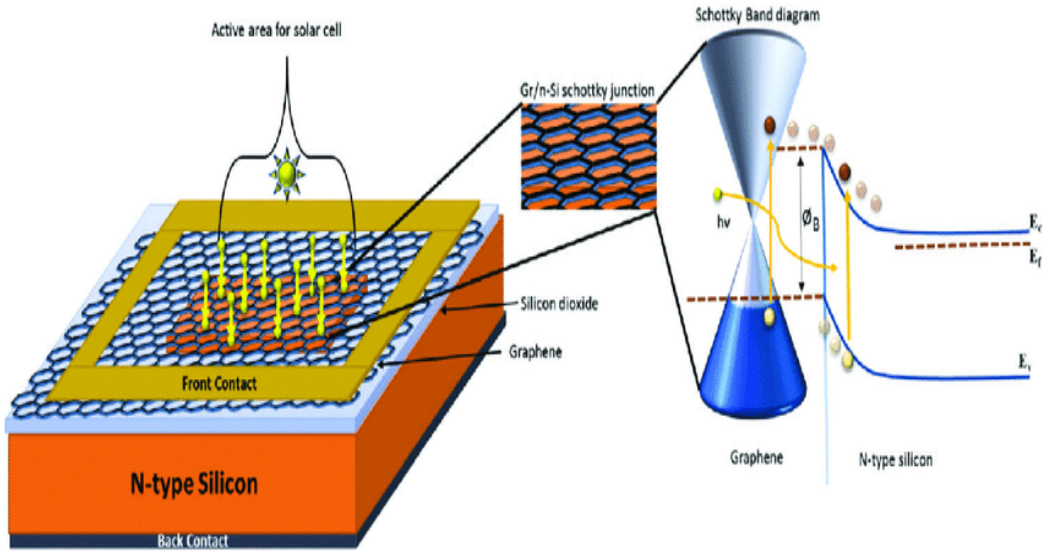

Figure 1.13: Schematic diagram of a conventional Gr/Si heterojunction solar cell. Energy band diagram of a Gr/Si heterojunction solar cell under illumination[28].

A built-in electric field separates incoming light from the electron–hole pairs created in Si as it travels across a junction. The holes move to the graphene side, while the electrons migrate to the n-type Si side, leading in current and power generation. In graphene/Si solar cells, the built-in potential ΦSBH is determined by the mismatch between the graphene work function G and the n-Si electron affinity χSi. To maximize electron and hole separation and collection in graphene/Si solar cells, we have more freedom in device design since graphene's function may be adjusted, as a result of which the potential drop over the depletion width is higher, allowing more efficient collection of carriers. The primary characteristics used to determine the efficiency of a solar cell are V_{OC}, I_{SC}, FF, and PCE. The third chapter delves into this topic in depth.

1.11 Optimization of Gr/Si heterojunction

PCE of the very first Gr/Si cell was recorded very low which was below requirements for industrial application about 1.5% [29]. Poor performance was reported due to factors such as pure graphene's very low work function (4.4eV) and high sheet resistance [30]. Afterwards verity of methods was introduced to adjust the work function of graphene and reflectance of Silicon wafers. Which were chemical doping, using multi-layer graphene and using interfacial layers. These methods helped optimizing performance of solar cell significantly.

Chapter 2

Synthesis Techniques

2.1 OXIDATION OF SILICON

In the process of making silicon-carbon hetero junction we need to add an insulating layer on the top of silicon, which can be easily done by oxidation of silicon from the top which results in formation of SiO_2 which is an excellent insulator and can also be used as masking of sacrificial layer. Dry oxidation and wet oxidation are the two most common ways for creating oxide layers. Both techniques rely on high-temperature furnaces, spanning from 800°C to 1200°C. It is possible to precisely regulate the oxygen flow within the furnace using either method. Only oxygen diluted with nitrogen comes into contact with the wafer surface in dry oxidation, but in wet oxidation, water vapour is present. The chemical mechanisms for dry and moist oxidation are as follows: The following are the dry and moist oxidation processes, respectively:

$$Si + O_2 \rightarrow SiO_2 \text{ (DRY)}$$

$$Si + 2H_2O \rightarrow SiO_2 + 2H_2 \text{ (WET)}$$

Using dry oxidation has the advantage of generating a highly pure oxide. Wet oxidation using water vapour increases the reaction rate dramatically, allowing for quicker development of thicker oxides. The resultant wet oxidation oxide layers are of lesser grade than the oxides produced by dry oxidation. As a result, dry oxidation is preferred for high-quality oxides, for thick oxide coatings, moist oxidation is recommended. The thickness of an oxide layer is generally measured in the range of 100 nm to 1.5 μm [31].

2.1.1 Oxidation Kinetics

For determining the relationship between oxide thickness and reaction time, Deal-Grove oxidation kinetics model is the most commonly employed. In

the model, oxygen mass transport through the oxide layer is explained by an ordinary differential equation solution.

$$x_{ox} = \frac{A}{2}(-1 + \sqrt{\frac{4B}{A^2}(t + \tau) + 1}$$

Where t denotes the oxidation period, A and B are temperature constants, and is a parameter determined by the initial oxide thickness xi.

2.2 COATING TECHNIQUES

2.2.1 Chemical Vapor Deposition (CVD)

Chemical vapour deposition (CVD) is a technique in which molecules are heated and transformed to a gaseous state (precursor), with the vapours then depositing on a particular substrate at a high temperature. Graphene is usually deposited on transition metal (TM) substrates, but it also relies on the type of precursor employed, such as Cu [32], Ru [33], and Ni [34]. On diverse TM substrates, Different hydrocarbons were decomposed to deposit graphene, including methane, benzene, acetylene, and ethylene [35]. Camphor (a white translucent solid with the chemical formula C10H16O) was utilized as a precursor material in the first effort to develop graphene on nickel surface in 2006 [36]. As Diagram of CVD is shown in Figure.2.1

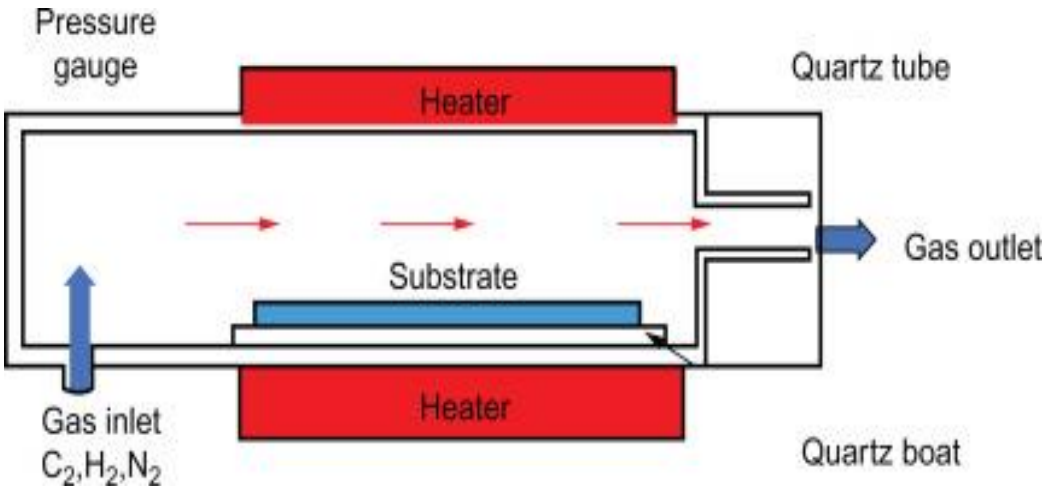

Figure 2.1: Chemical Vapour Deposition [37]

2.2.2 Electrodeposition

When metal ions in solution are electrochemically deposited onto a substrate, the process is known as electroplating or electrodeposition. This method is frequently used in MEMS devices to deposit copper and magnetic materials. Surface quality and roughness are lower in electrodeposited films than in films produced by physical vapour deposition. Film uniformity can be a concern, but it can be addressed by carefully controlling the applied electric current [31].Figure 2.2 shows the mechanism of electrodeposition in which Pt is being deposited on GDL electrode.

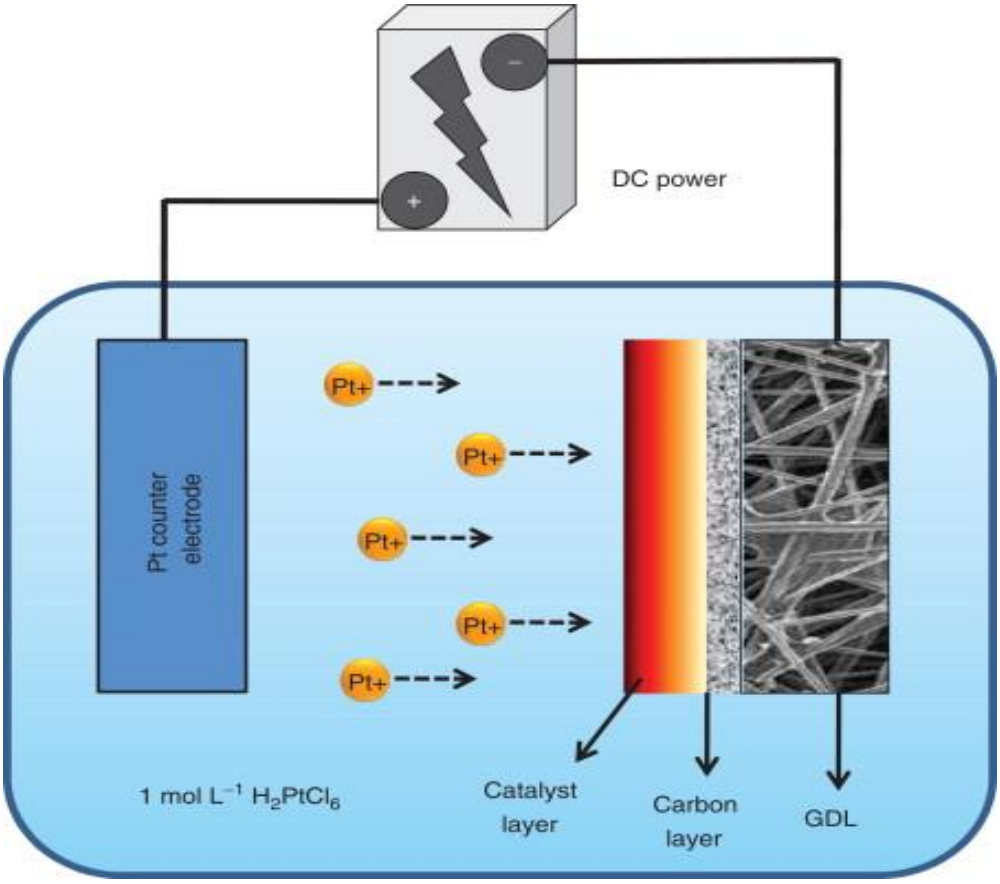

Figure 2.2: Electrodeposition [38]

2.2.3 Spin casting

It is possible to add certain materials to a substrate by dissolving them in a solution, putting them to a wafer, then centrifugally rotating the wafer in order to disperse them evenly across its face. The wafer is then heated to evaporate the solvent and reveal the thin layer below. The technique is also known as spinning. Sol-gels are spin-cast colloidal fluids containing solid polymer particles. When it comes to applying photoresist on wafers, spin casting is the method of choice [31]. Block diagram of spin casting setup is shown in figure 2.3.

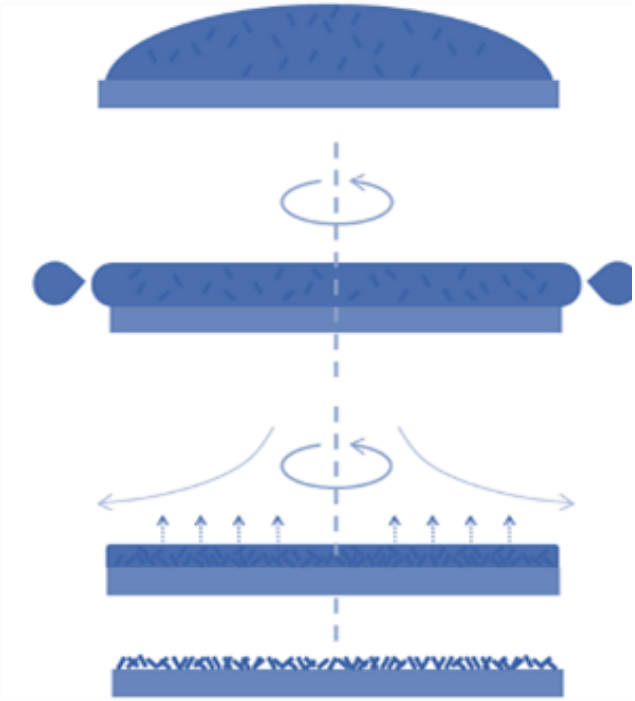

Figure 2.3: spin casting

2.2.4 Etching

Etching is a process of chemically removing material to make physical structures. There are basically two types of etching techniques Wet chemical etching and Dry etching.

2.3 PHOTOLITHOGRAPHY

Photolithography is an optical printing process. It is used for the purpose of adding layers onto the substrate. It this process a photosensitive material is used as photoresist, which if exposed to the light becomes less soluble or more soluble. Then a mask is created using transparent material with selective opaque region, with the help of mask only selected region is exposed to light. After the exposure to light a developer is used which etches the exposed or unexposed region as per requirement and wanted pattern of photoresist is left behind on the substrate as shown in Figure 2.4. [31].

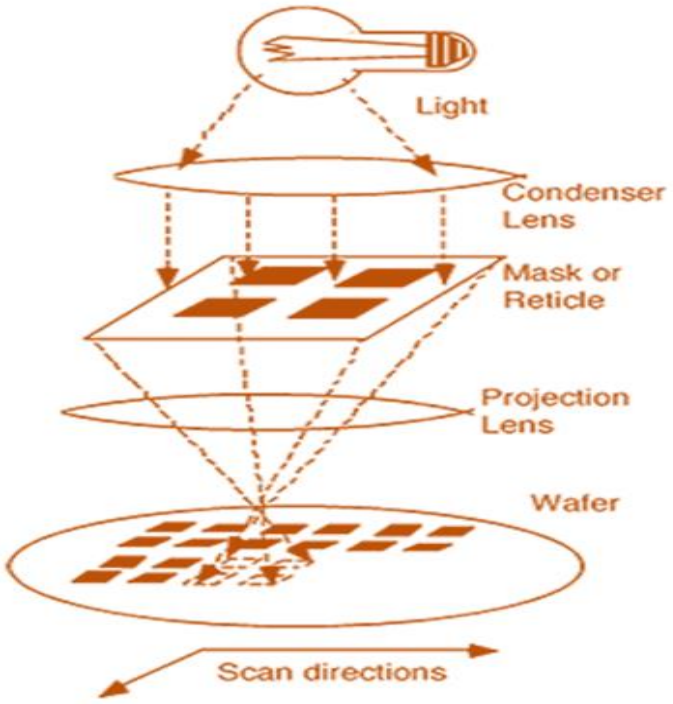

Figure 2.4: Photolithography Schematic.

2.4 METHODOLOGY

Substrate of Si (100) was thermally oxidized at 1000°C for 6h in order to grow 300nm thick layer of SiO_2, after oxidation back contacts of Al were made by thermal evaporation. Photolithography was used to fabricate the front window of the device using positive photoresist and desired area was etched by using HF (1:10). Front metallization of Au was also done with the help of photolithography and thermal evaporation. Graphene was transferred onto the substrate and finally QDs were coated by using the spin coater. Figure 2.5. shows the graphical mechanism of the proposed methodology.

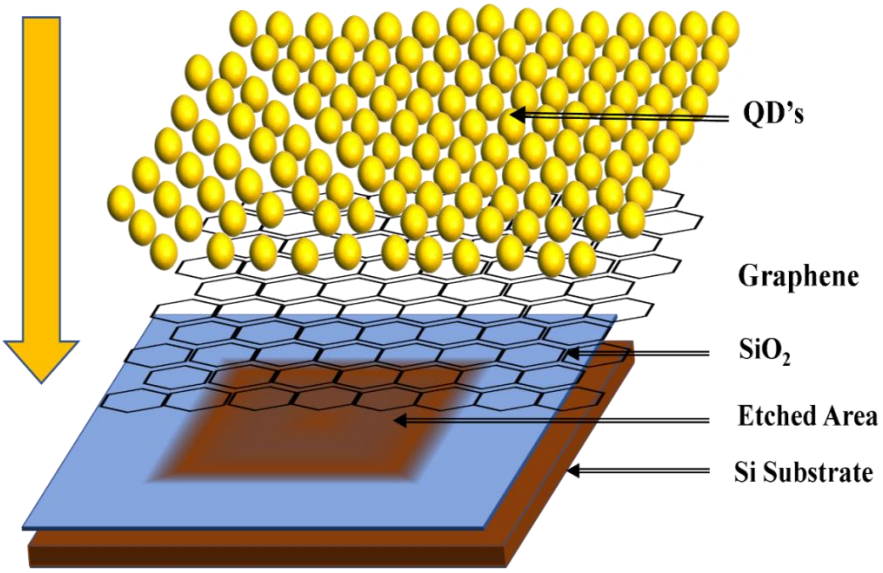

Figure 2.5: Schematic

Figure 2.6 shows 2D Diagram of the fabricated device.

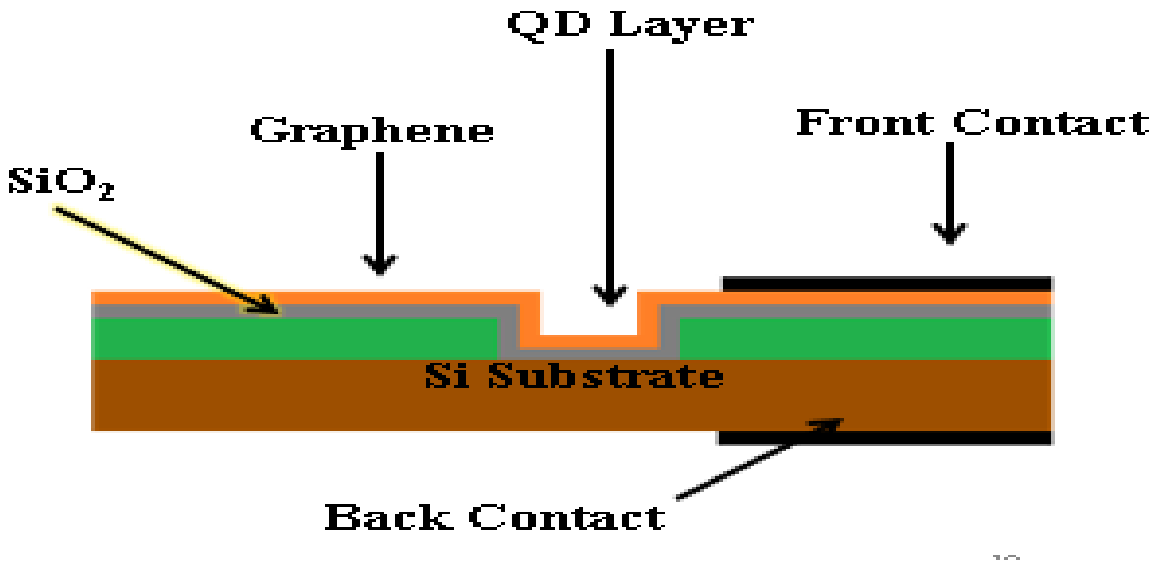

Figure 2.6: Fabricated Device

Flow chart of the proposed methodology is shown in figure 2.7. Etching was done by chemical etching process. While transfer of graphene was performed by the method explained in the research paper by Alfonso Reina [39]

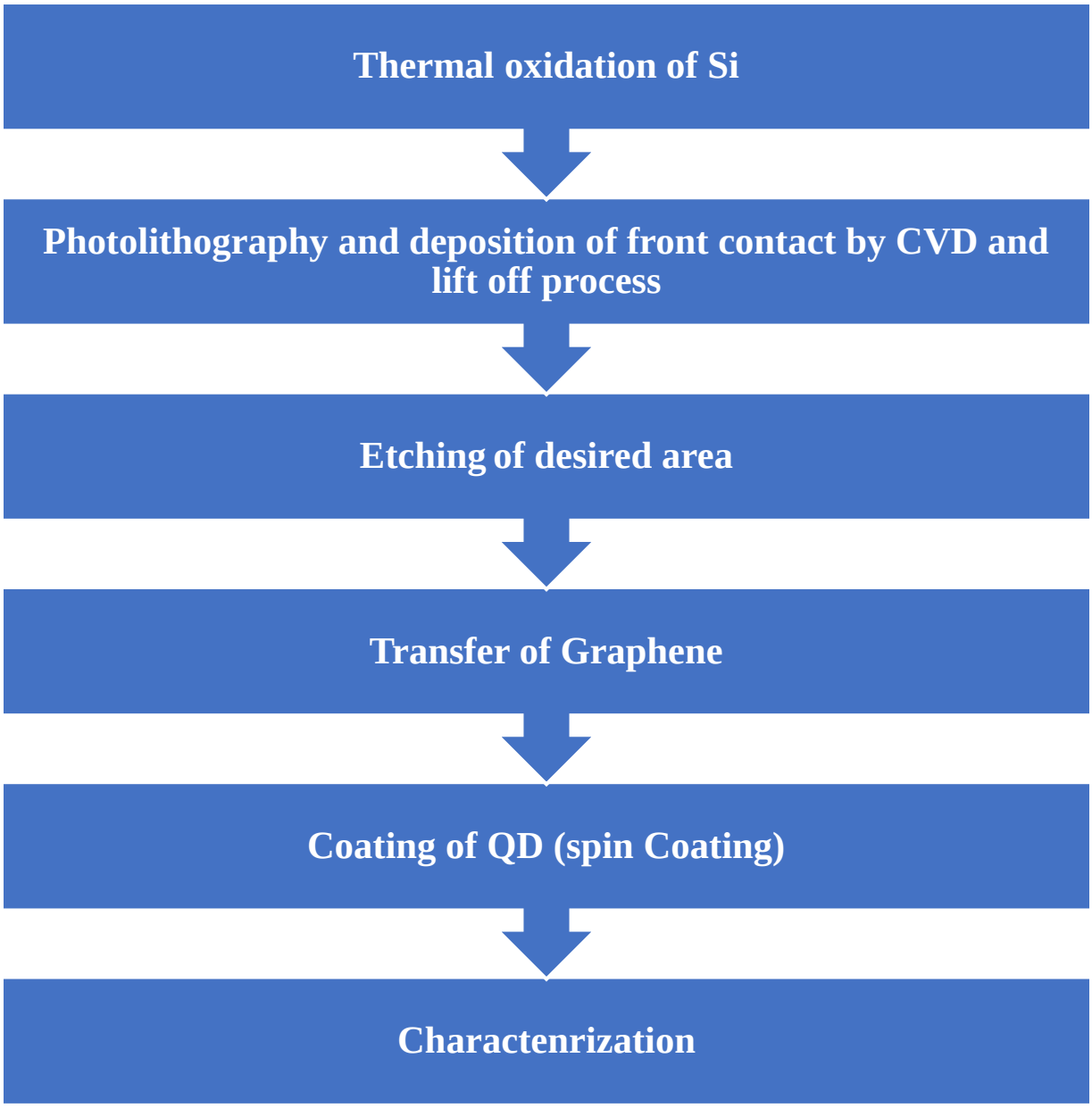

Figure 2.7: Flow Chart of Synthesis

Chapter 3

Characterization Techniques

3.1 Atomic Force Microscopy:

Atomic force microscopy (AFM) is a scanning probe microscope with a high-resolution capability. AFM is basic method for measuring the topological images, force and manipulated matter at nanoscales. AFM measures force by measuring the attraction and repulsion forces between the tip and the sample surface. In AFM working principle a probe (tip) is attached to the end of a cantilever which moves up and down in response to force reaction. The tip is usually made of silicon and silicon dioxide with precise size. When a tip touches the surface of a sample cantilever show some deflection obeying the Hooke's law which responded force of attraction or repulsion. The deflection of cantilever is detected by a beam of laser and photodiodes [40]. A simple block diagram of a typical AFM diagram is shown in Figure 3.1.

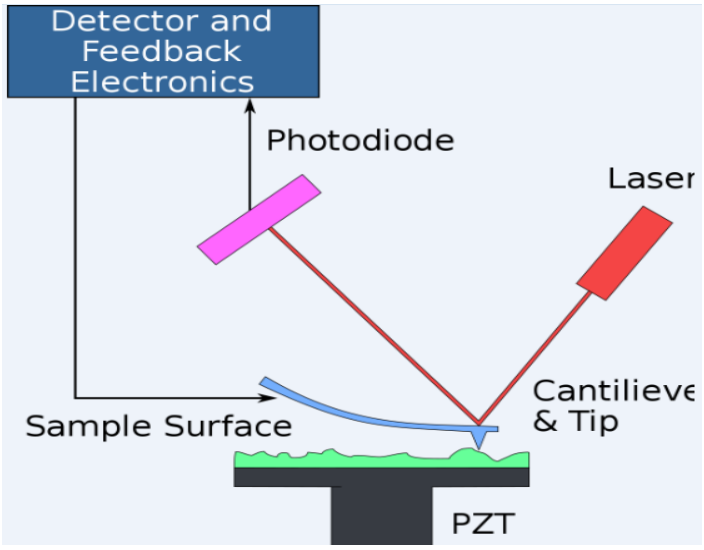

Figure 3.1: Block diagram of AFM setup.

3.2 RAMAN SPECTROSCOPY:

In 1928 sir C.V. Raman has got noble prize as the founder of phenomenon of Raman spectroscopy. In this phenomenon photon are scattered in-elastically that means frequency of emitted photons changes when a light of source fall on a material. So, the basic principle of Raman scattering depends upon the energy shift between the incident and scattered photons. Setup is shown in figure 3.2. The Raman Effect describes the up or down shift in frequency of reemitted photons in contrast to the initial monochromatic frequency. In atoms, the Raman Effect provides information on vibrational, rotational, and other low frequency transitions.

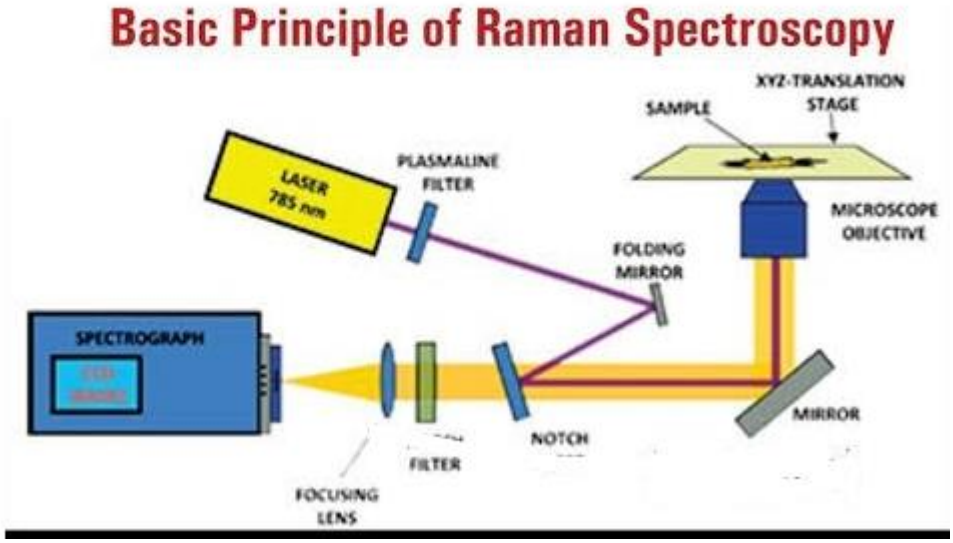

Figure 3.2: Raman spectroscopy working principle.

By this technique the structure, crystallinity and defect of synthesized materials can be determined. When a material is irradiated by a source of light the atom and molecules of this material get excited and show transitions from ground state to excited state. Thus, there are two possible consequences obtained from Raman scattering, stokes and anti-stokes scattering. In stokes scattering, the incident photons energy is less than the scattered photons. When the incident photons energy is greater than

scattered photons it's called anti-stokes scattering as shown in figure 3.3 [41].

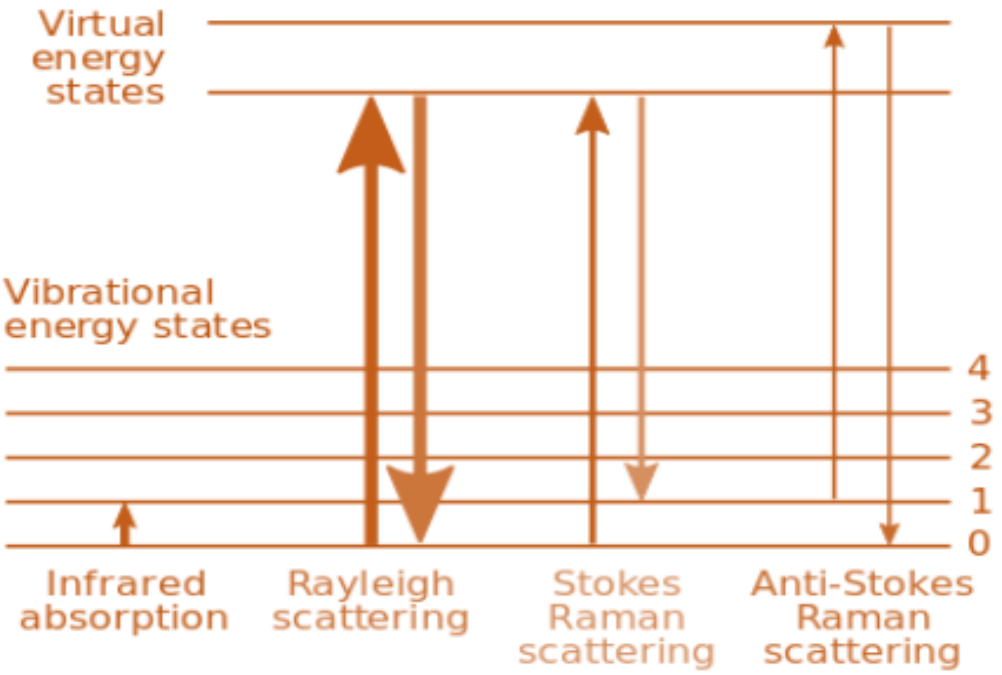

Figure 3.3:An inelastic scattering of stokes and anti-stokes processes.

When de excitation of electron from conduction to valance band occurs, light excreted from a material which is called luminescence. Luminescence has many kinds, likewise photoluminescence, electroluminescence, cathode luminescence and Bioluminescence.

3.3 PHOTOLUMINESCENCE:

In photoluminescence process when a light source interacts with matter it emitted photo light which occurs by photo excitations. When an external source of light is incident on the material, electron moves from conduction band to valance band leaving holes behind it. Photoluminescence follows three step processes: Excitation, recombination, and heat balance. The electron-hole pair recombines and produces photons after heat balance. Quantized energy band gap generates by defects states and impurity atoms. Every state corresponds to a particular energy and after recombination

produces a photon of that energy. There are two types of electron-hole pair recombination. In irradiative recombination, a photon produced with specific wavelength. In non-radiative recombination, a heat loss, phonon vibration, or any mode of energy loss can occur which do not emit any photon as shown in figure 3.4[42].

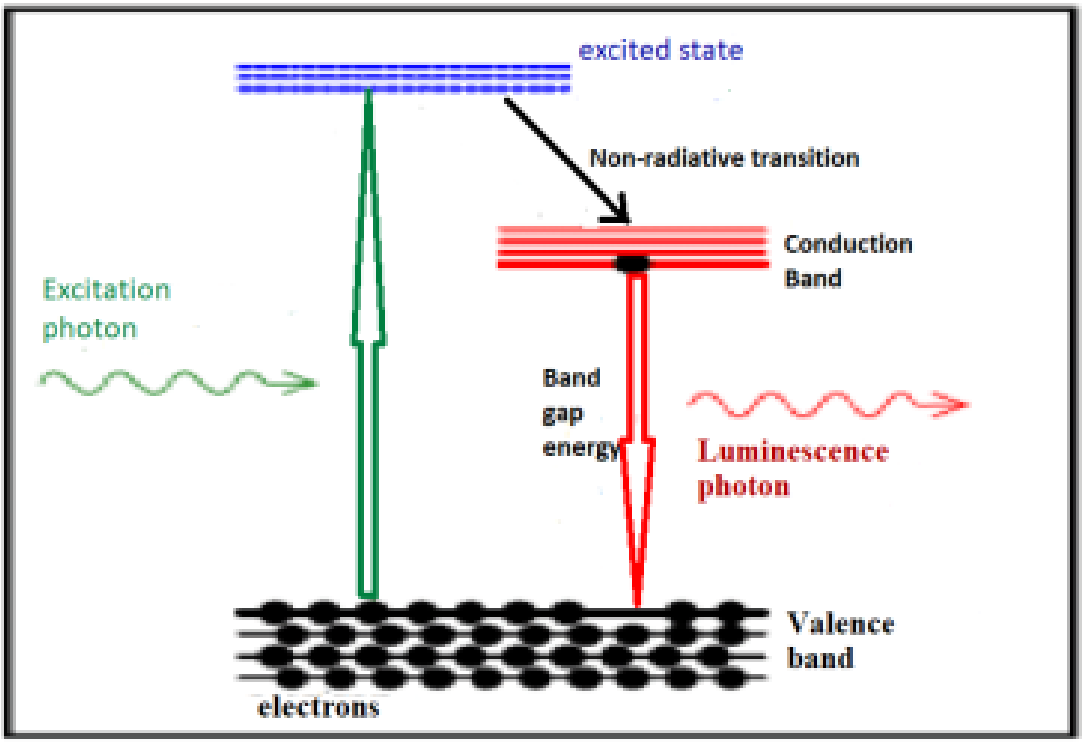

Figure 3.4*:* Energy diagram showing PL phenomenon.

Figure 3.5 shows mechanism of PL spectroscopy which is a nondestructive characterization technique for studying the electronic band structure of materials, and it is widely regarded as the best approach for determining luminescence characteristics and defect states.

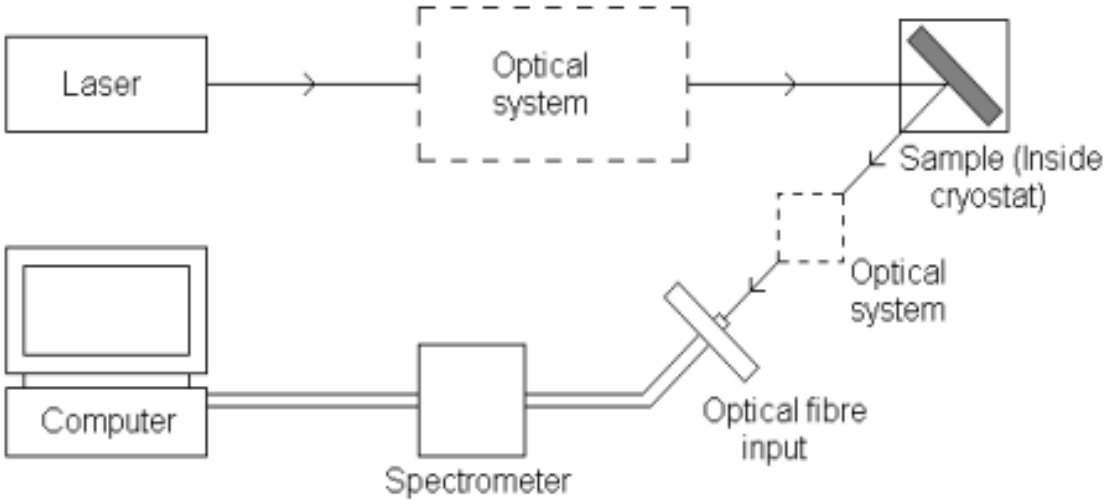

Figure 3.5: Basic principle of Photoluminescence.

3.4 IV CHARACTERIZATION

IV graph is basically used to check the ohmic behavior of the devices. In cases of solar cells, it is used to analyze the current and voltage variation and for the calculation of efficiency. Basic solar cell characteristics such as short circuit current, open circuit voltage, ideality factor, barrier height, series, and shunt resistance may also be found using the IV curve. IV setup is shown in figure 3.6.

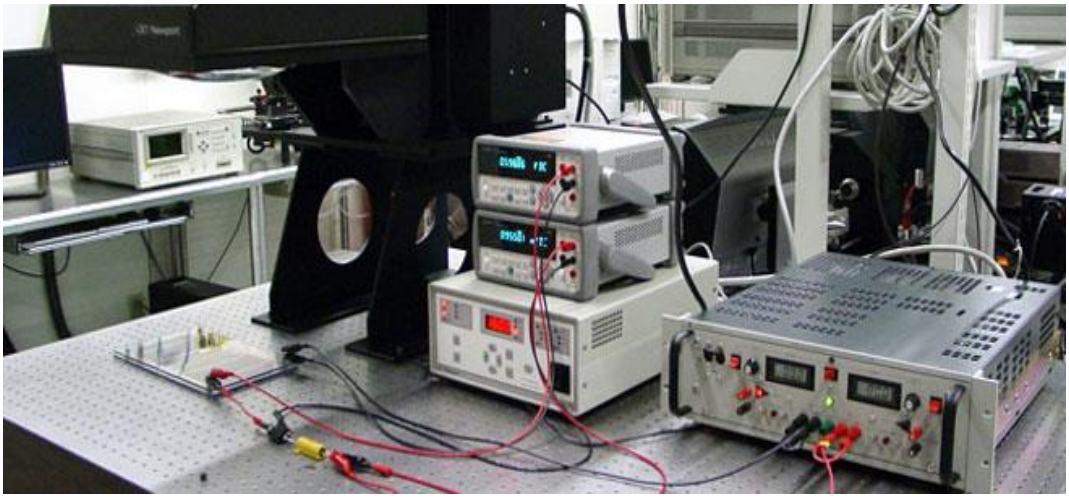

Figure 3.6: IV Setup

3.4.1 Short circuit Current

The current created by a solar cell when the voltage across the cell is 0 is known as short circuit current. It's typically denoted by Isc. The creation and collecting of light-generated carriers causes the short-circuit current. The short-circuit current and light-generated current are identical in a perfect solar cell with relatively minor resistive loss mechanisms. As a result, the shot-circuit current is the highest current that a solar cell can produce [43]. The current in a short circuit is determined by the following parameters.

- Solar cell area
- Photon count
- Spectrum of incoming light
- Optical characteristics

3.4.2 Open circuit voltage

The open-circuit voltage, or VOC, is the highest voltage a solar cell can generate while the current is zero. Due to the bias of the solar cell junction with the light-generated current, the open-circuit voltage indicates the forward bias on the solar cell. Figure 3.7 shows solar cell parameters.

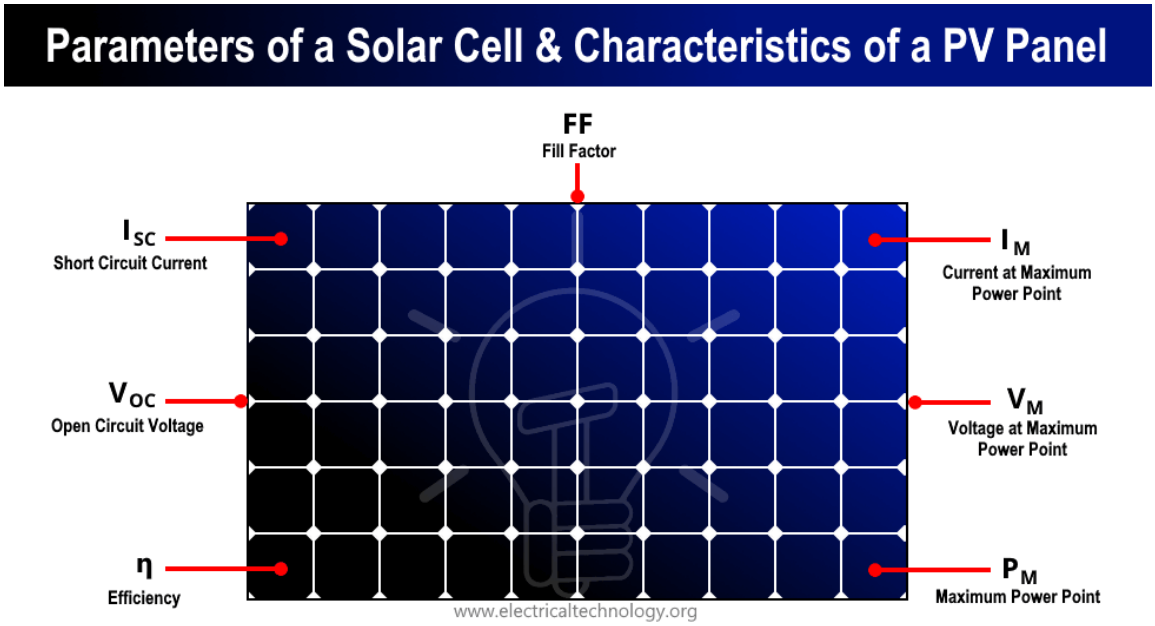

Figure 3.7:Solar Cell Parameters

3.4.3 Ideality Factor

A diode's ideality factor is a measurement of how well it matches the ideal diode equation. $n = \frac{q}{kt}(m)$ Equation 3.1

Ideality factor and flat band voltage which is calculated from CV is used to observe the electrical properties of the material.

Chapter 4

Results and Discussion

4.1 Optical Microscopy

Optical microscope was used for close images of the fabricated device. We used the 10x lens for the optical photographs.

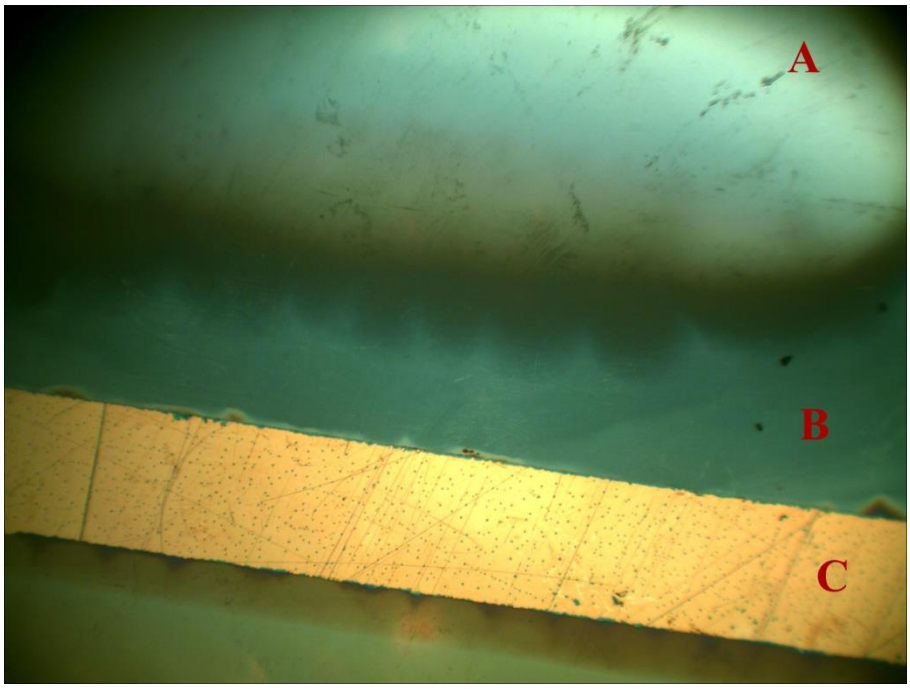

Figure 4.1: Sample 1 Optical Picture

In the figure 4.1 and 4.3 patch, A, shows the Bare Silicon Surface where SiO_2 has been etched. This is where Graphene will come in contact with Si and Produce a Gr/Si heterojunction while at B the SiO_2 surface is unetched and it is used as an insulator. The Gold coating at C is gold contact which is used as a front contact for solar cell. While in figure 4.2 picture of a half-fabricated cell is shown. In this state photoresist is coated in the cell which helps in lithography and etching of desired patch. Patch A is to be etched away in order to obtain bare Si surface.

While Patch B and C are to be remain as it is. Photoresist is then removed by Aceton.

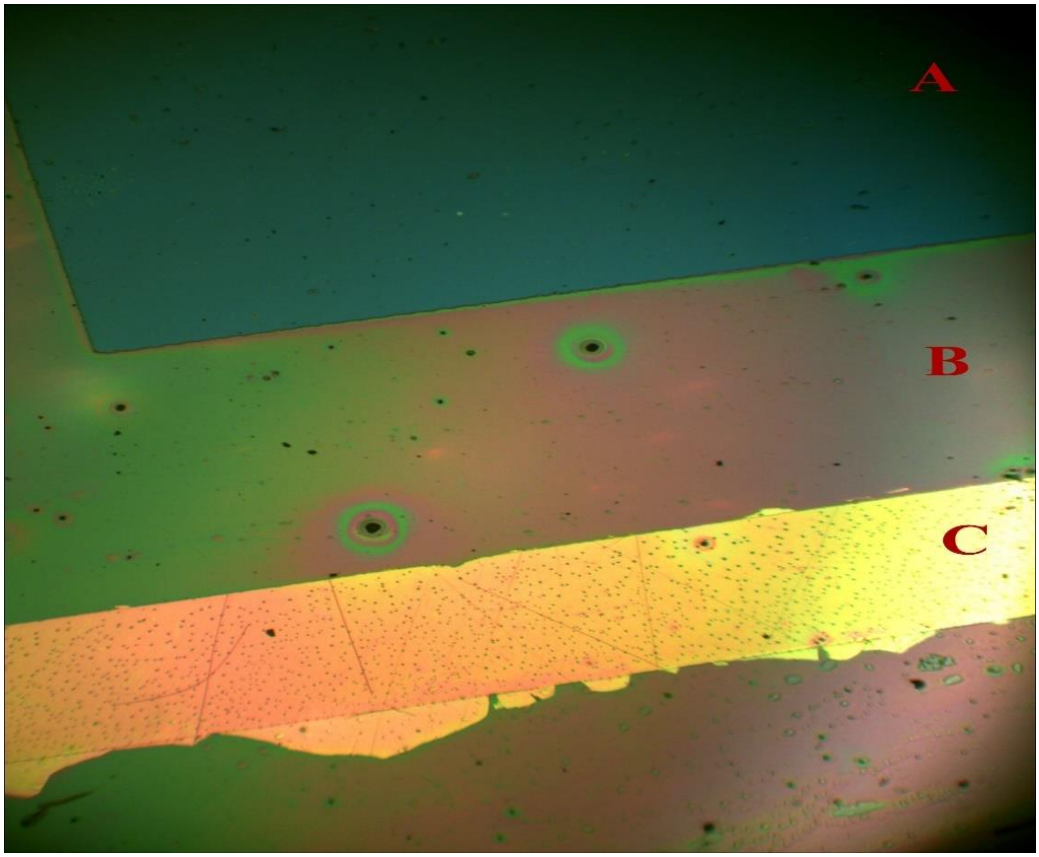

Figure 4.2: Optical Microscopy of Half-Done Sample

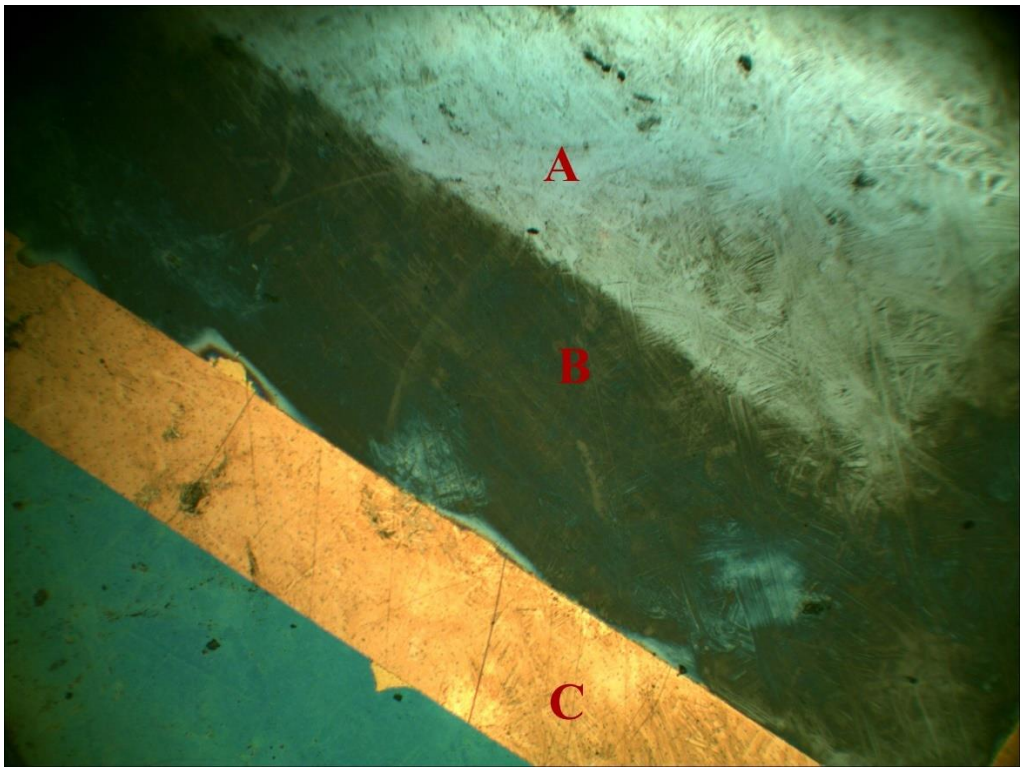

Figure 4.3 Optical Microscopy of Sample 2

4.2 ATOMIC FORCE MICROSCOPY

AFM was used to determine the surface roughness and the comparison of graphene and coated quantum dots. Below figures shows the AFM 3D view of the Sample 1 and Sample 2 before the coating of graphene with average roughness of 113.7 nm and 106.9 nm respectively. Below picture of AFM were taken after the coating of Quantum Dots, below pictures have a significant variation in roughness parameter which shows the presence of Quantum dots. Though quantum dots were not distributed uniformly but the roughness is better as compared to bare graphene.

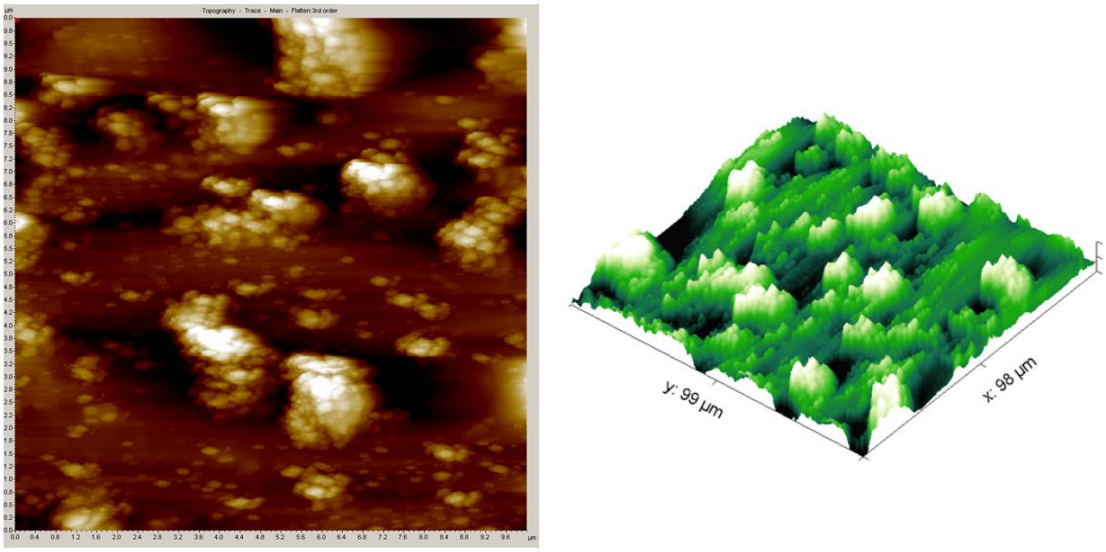

Figure 4.4: S1 pristine graphene

After the coating of QD's the roughness increased which was 112nm for S1 and 116nm for S2. This shows the presence of QD's.

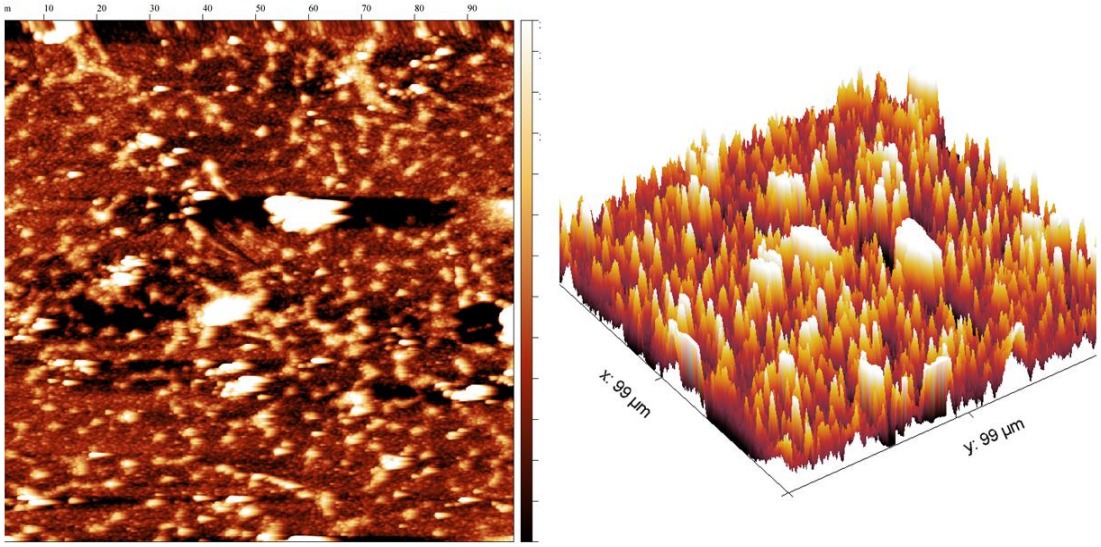

Figure 4.5: S1 Qds

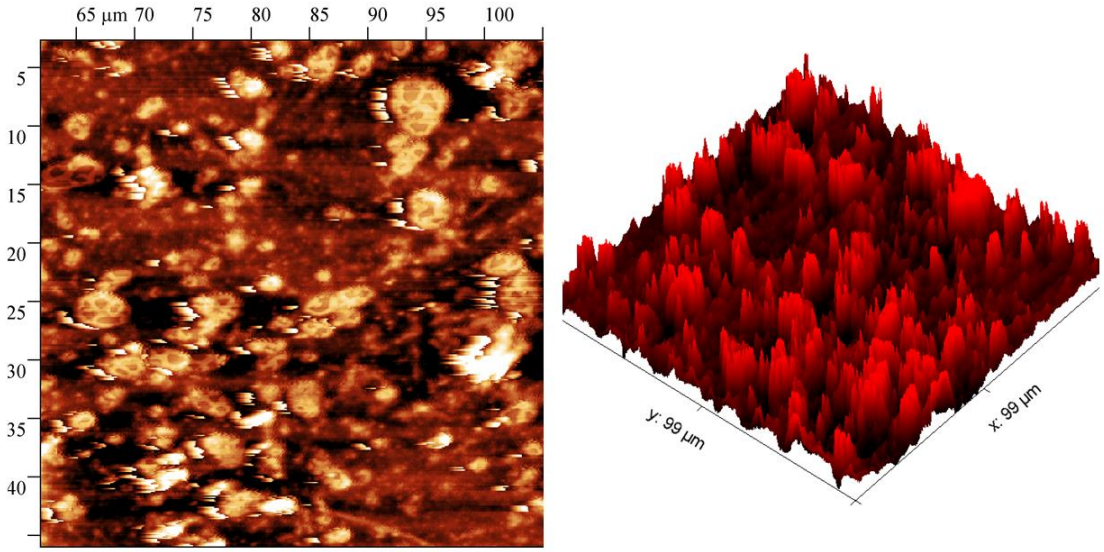

Figure 4.6: S2 pristine Graphene

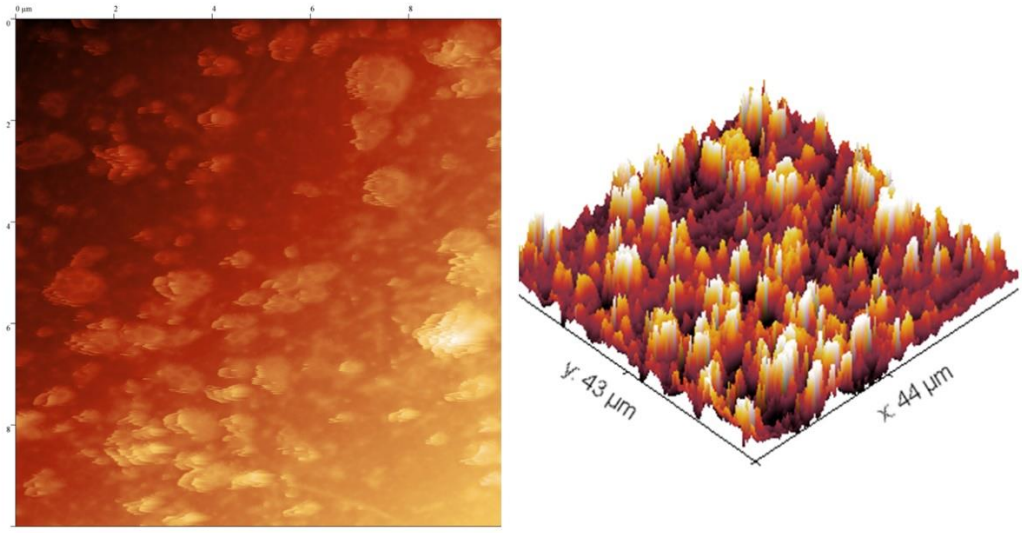

Figure 4.7: S2 Qds

4.3 RAMAN SPECTROSCOPY

We used Raman spectroscopy to determine the Graphene thickness and other parameters. In the Raman spectroscopy of Graphene, G- band is at 1596 cm^{-1}, D-band is at 1366 cm^{-1} and 2D-Band is at 2719 cm^{-1} position these are the signature modes of the graphene. Ratio of Id/Ig gives information about defects in the surface of graphene, which in our case is 0.29. such low ratio tells us about that the graphene has very less defects. 2D band represents 2D materials and it is overtone of D-band. Ratio between I_{2D} and I_G tells us about the numbers of graphene layer which in our case is 2.4, which represents that it is a monolayer of graphene.

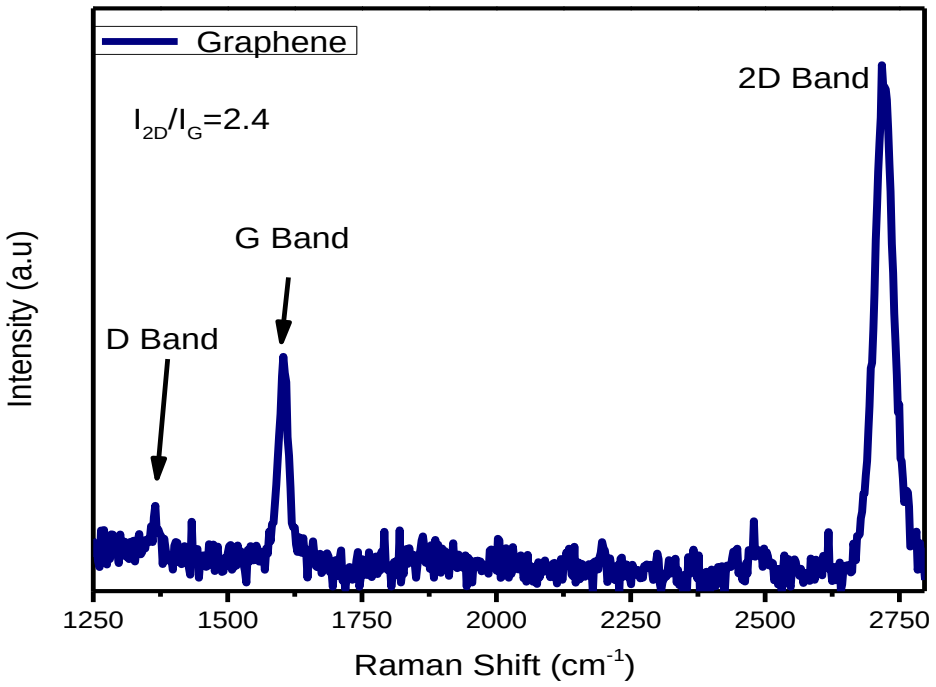

Figure 4.8: Raman Spectroscopy

4.4 PHOTOLUMINESCENCE

Photoluminescence was used to determine the emission wavelength of the QDs. Peaks at 527nm and 650nm were observed, peak at 527nm and 650nm refer to green and red lights respectively. Bandgap of peak at 527nm is 2.3eV and the peak at 650nm has bandgap of 1.9eV. As higher band corresponds to smaller size of quantum dots which is verified by the data sheet provided by the manufacturer of the quantum dots.

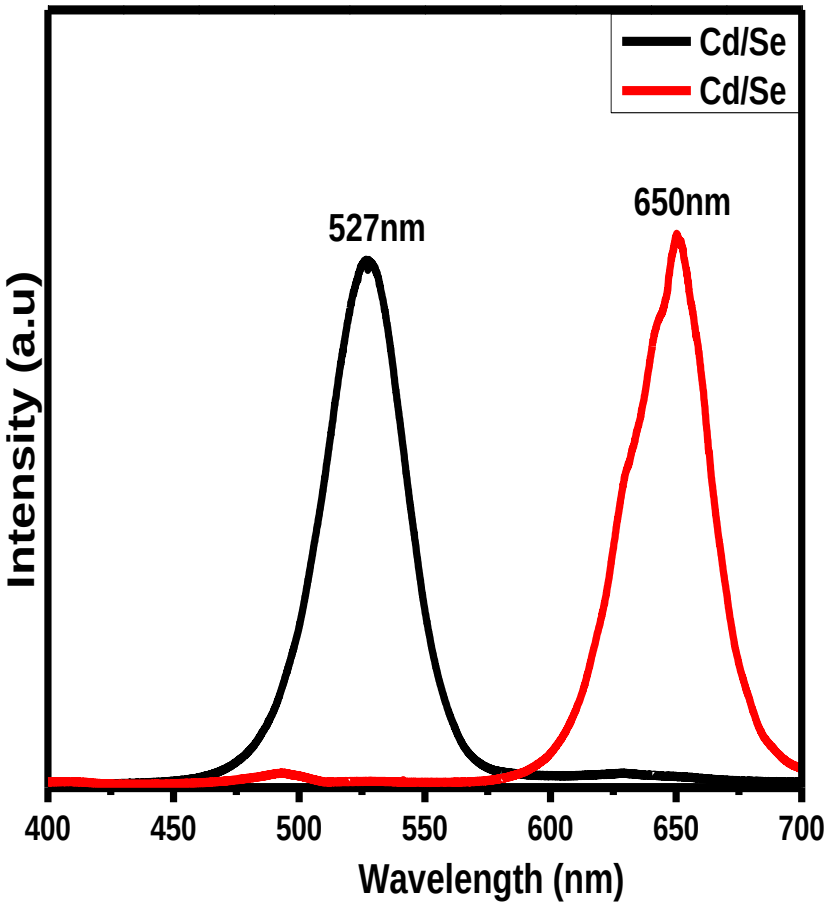

Figure 4.9: Photoluminescence

4.5 IV CHARACTERIZATION

Current Voltage graphs were used to study the ohmic behavior of the fabricated devices in light and dark situations. Also, to study the current generated by the solar cells. Graph below shows the IV curves of the different samples used in our research.

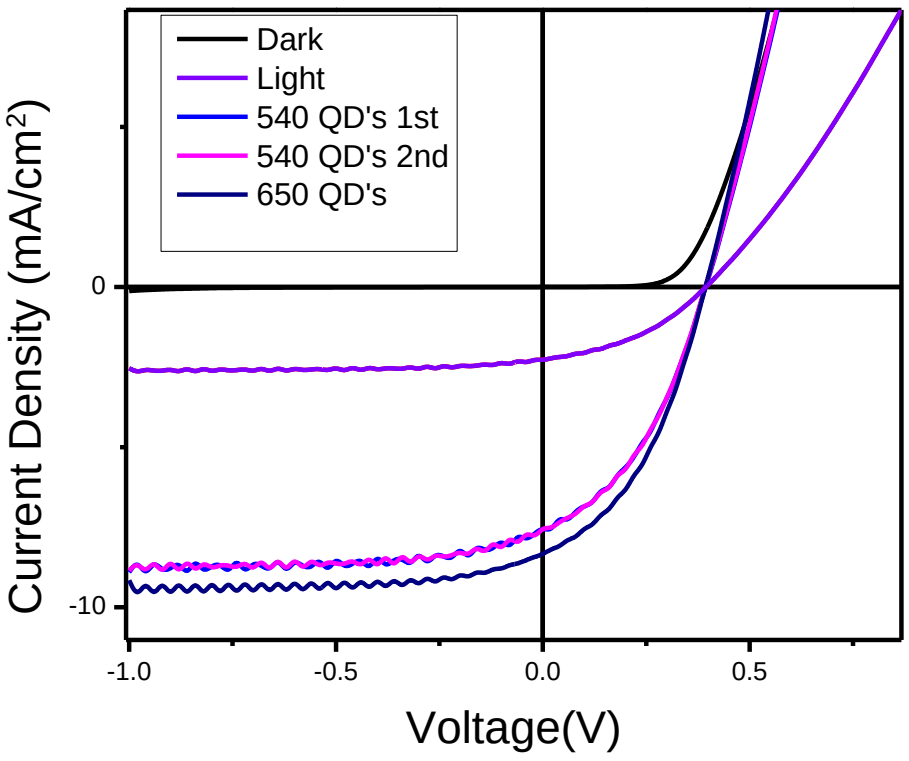

Figure 4.10: IV Curve

4.5.1 Ideality Factor

Ideality factor was calculated by plotting ln of dark current against voltage and then getting slop of the curve. Red line in the figures 4.8 and 4.9 show the area of slop(m). after putting value of m in equation 3 we found the ideality factor of 1.58 and 1.6 for sample 1 and sample 2 respectively.

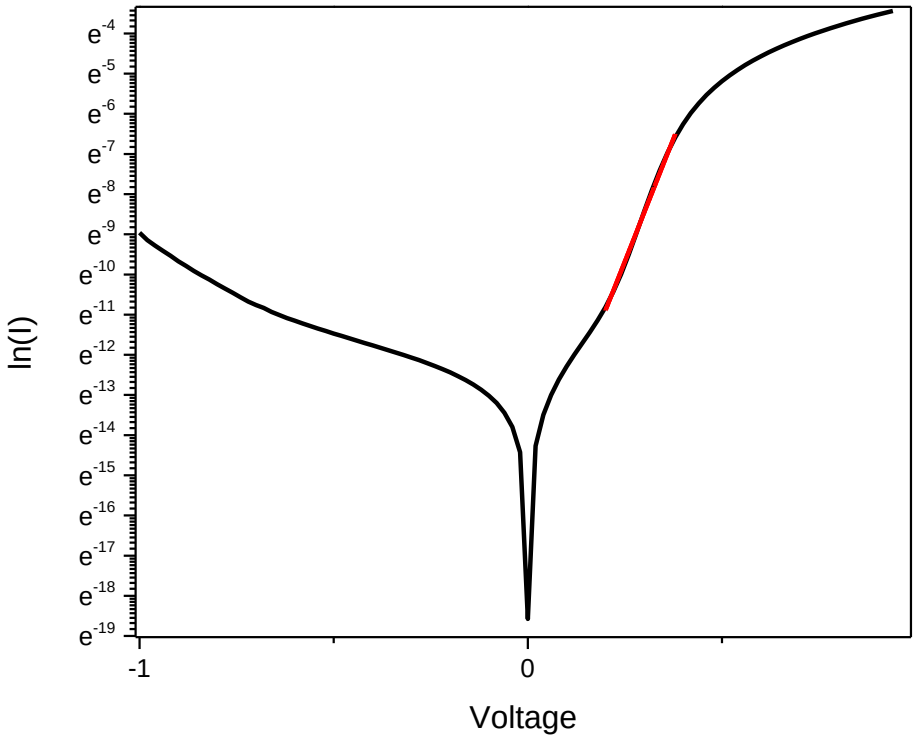

Figure 4.11: ideality factor calculation sample 1

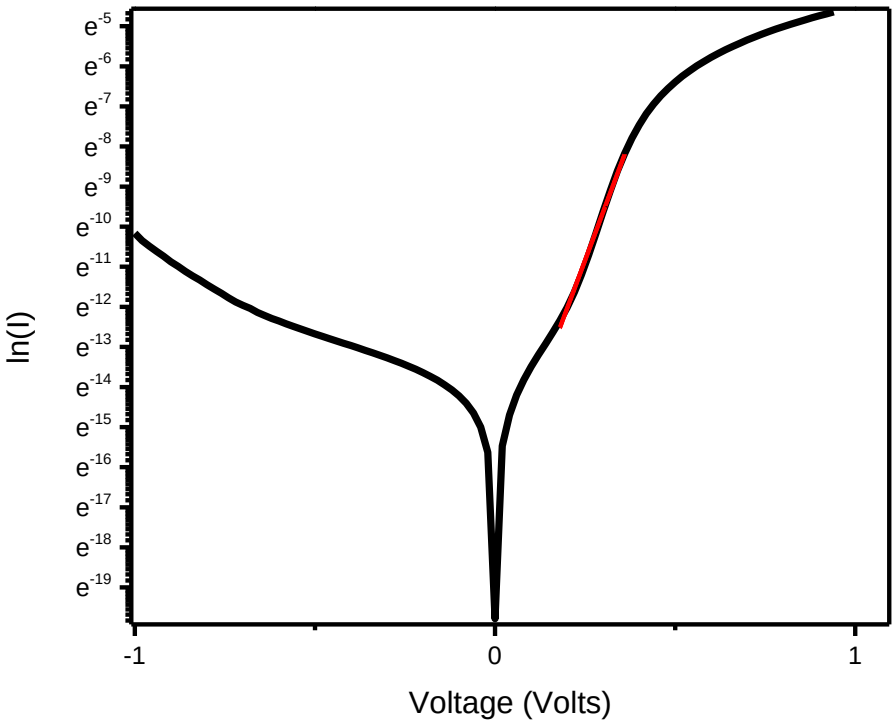

Figure 4.12: Ideality factor sample 2

4.6 FLAT BAND VOLTAGE

Capacitance and voltage graph were used to find flat band voltage with the help of Mott-Schottky Relation. For our sample the flat band voltage is near to ideal. For sample 1. Flat band voltage of 0.9V and for sample 2 flat band voltage of 0.7V was calculated.

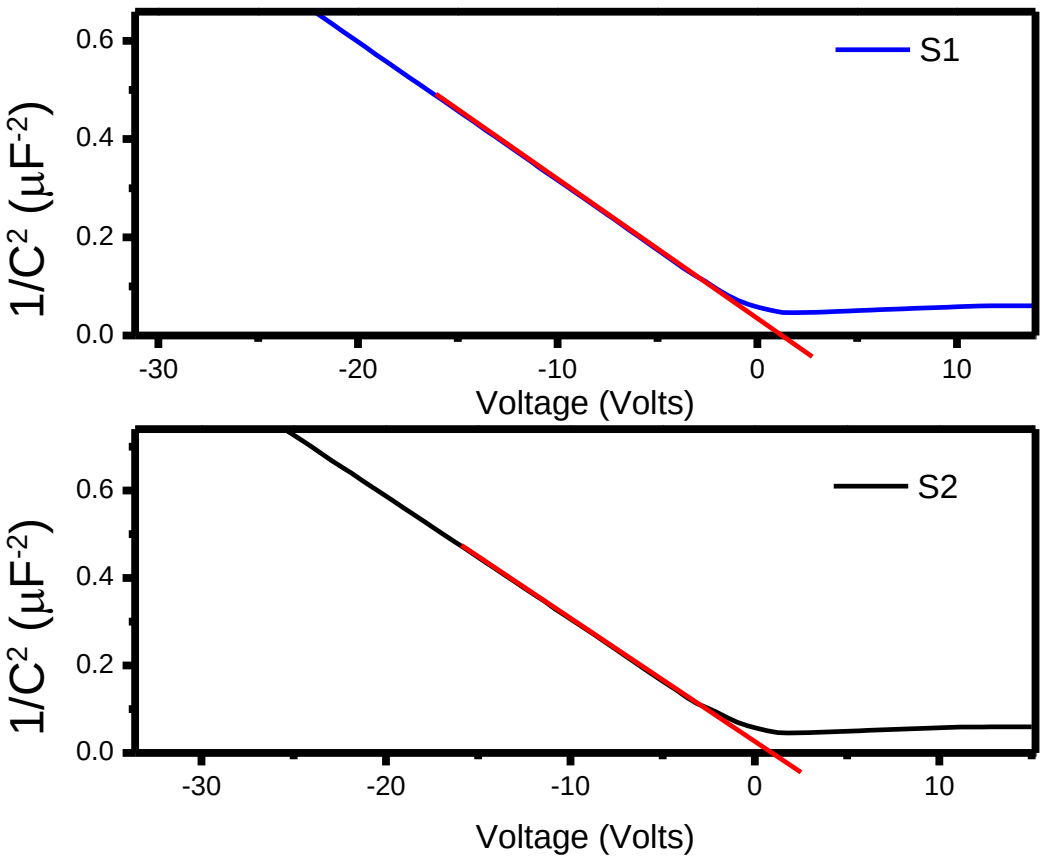

Figure 4.13: Flat Band Graph

4.7 EFFICIENCY CALCULATION

Figure 4.14 shows the IV graph of pristine graphene silicon heterojunction. After calculating current density and efficiency it is observed that the current density is very low (η=0.60, J=2.27mA/cm^2) which in our case was ideal because we were trying to enhance current density so due to low current density it was very easy to study the effect on current density.

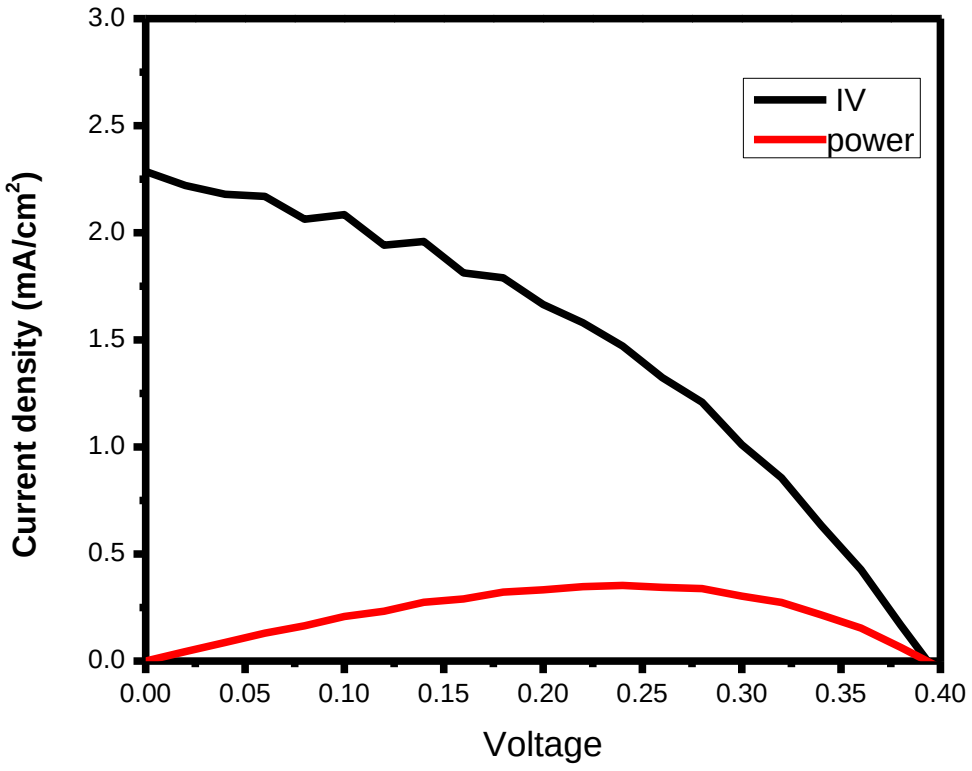

Figure 4.14:IV without QDs

Figure 4.15 shows the enhanced current density after the coating of QDs, J=7.57mA/cm^2. This shows our main objective to enhance current density is achieved. After the coating of QD's of 540nm emission a clear enhance is observed in the current density.

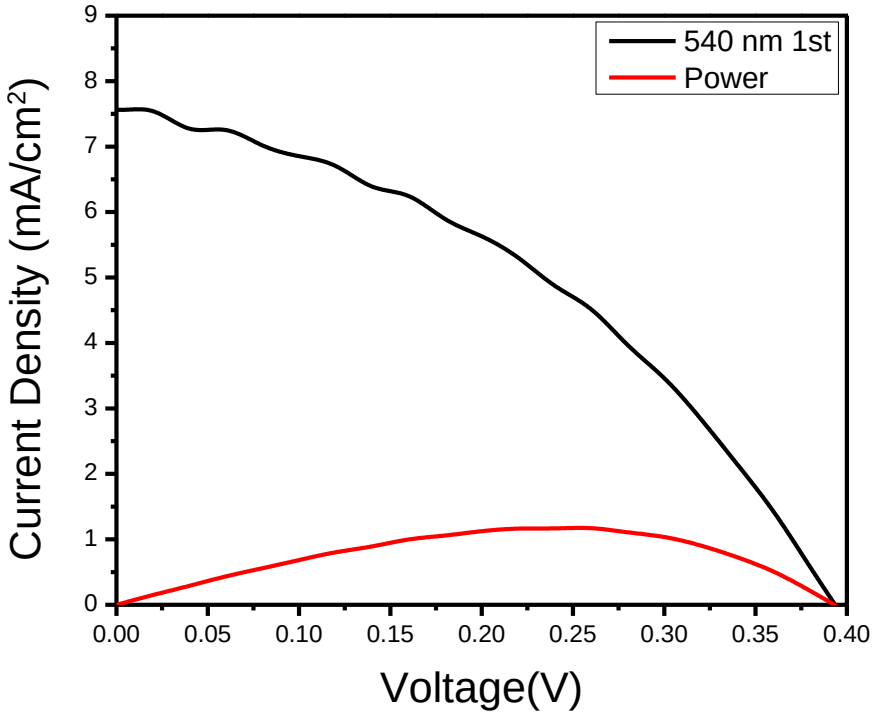

Figure 4.15: IV with 540 QDs 1st

For our first reading of 540nm QD's J_{SC}=7.57mA, V_{OC}=.39V was recorded. After further calculation efficiency was calculated to be 1.962% (Figure 4.13). for Second reading of 540nm J_{SC}=7.4mA and V_{OC}=0.39V was observed with the Efficiency of 1.97%.

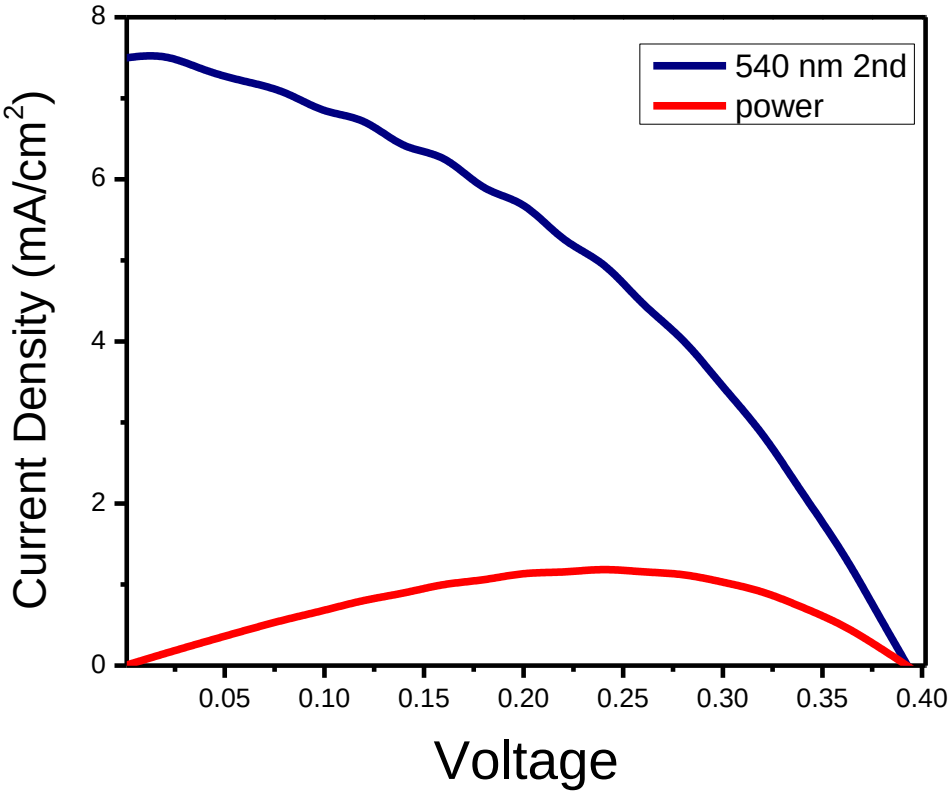

Figure 4.16: IV with 540 QDs 2nd

Coating of 650nm wavelength emitting QD's gave us a further boost in efficiency and current Density. With J_{SC}=8mA, V_{OC}=0.39V and efficiency was calculated to be 2.12%.

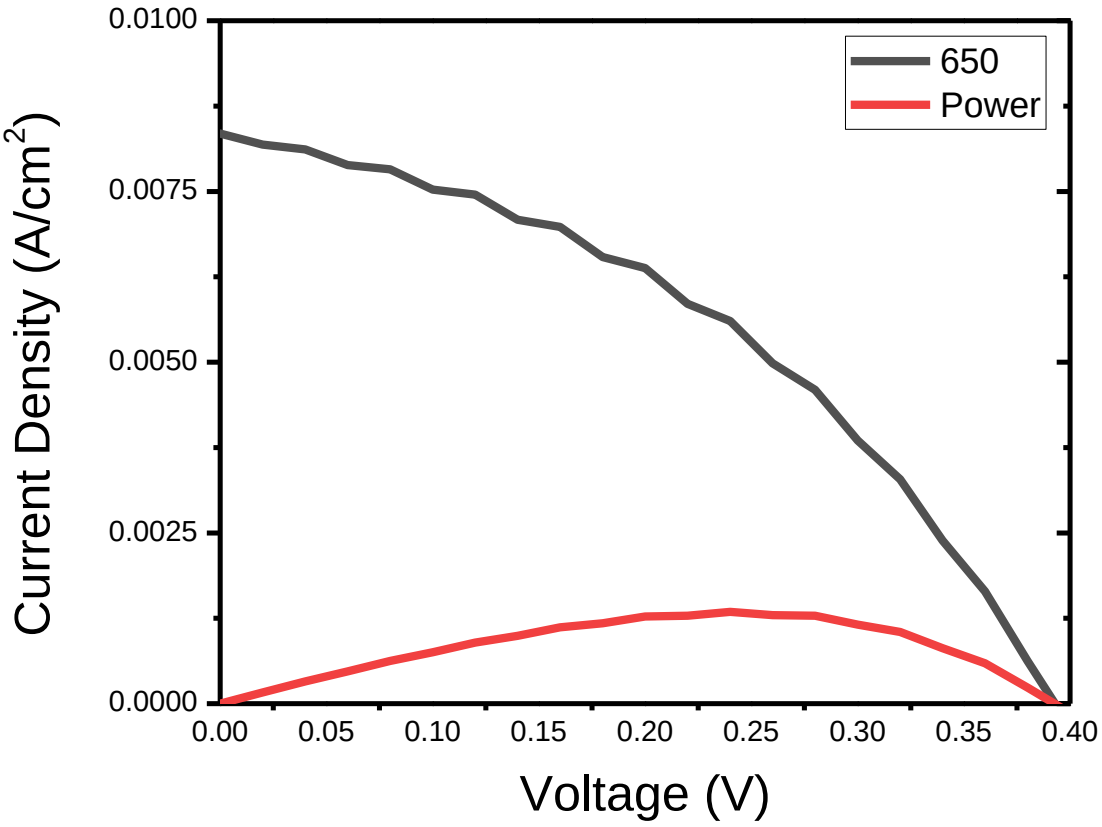

Figure 4.17: Efficiency calculation with 650 Qds

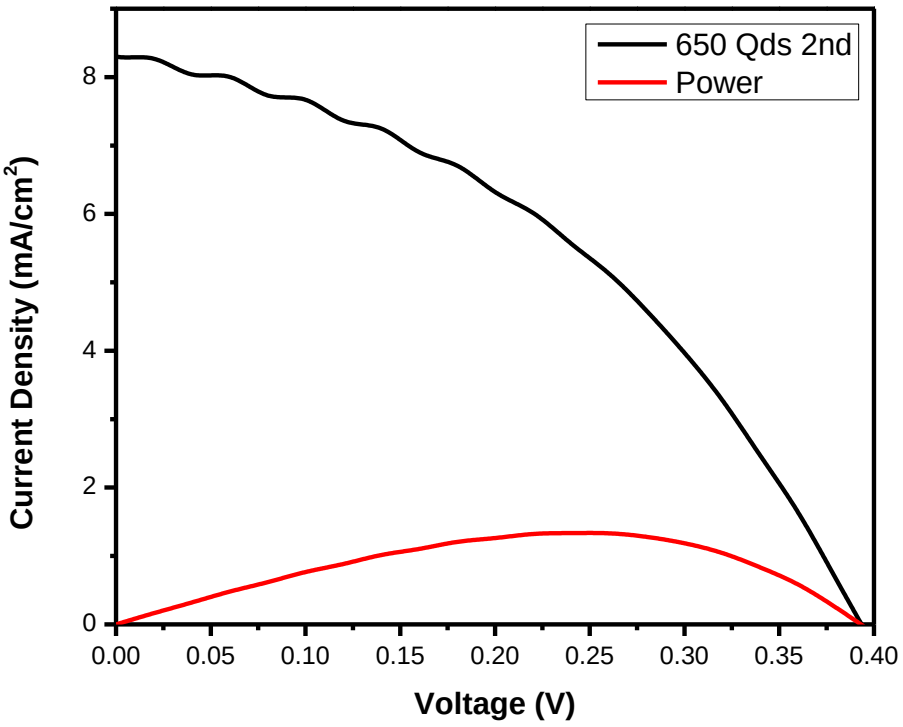

Figure 4.18: Efficiency Calculation with 650nm QD's 2nd reading

Conclusion And Recommendations

Research work represented in this thesis mainly focused on the enhancement of current density and the efficiency of graphene silicon heterojunction. Which previously observed to be very low as in the literature it was less the one percent with exceptional cases reaching above 1% [44]. To enhance the efficiency a new hypothesis was presented which was to coat this Gr/Si heterojunction with QD's which will help silicon absorb more photons and result in higher photo conversion efficiency.

Table 5.1: Comparison With litrature

Sample	**Efficiency %**	**Current Density (mA/cm^2)**	**Percentage Increase In Efficiency (%)**	**Reference**
Gr/Si	0.478	5.61	NIL	[44]
Gr/Si dopped	1.257	6.47	NIL	[44]
Pristine	0.60	2.27	125	Current Work
540 1st	1.96	7.4	410	Current Work
540 2nd	1.97	7.57	411	Current Work
650 Qds	2.12	8.0	443	Current Work
650 2nd	2.24	8.29	468	Current Work

Raman spectroscopy was done to find the thickness of graphene, which was calculated by I_{2D}/I_G ratio. It was confirmed that graphene deposited was mono-layer and has very less defects. Photoluminescence was performed to analyze

quantum dots and their emission wavelengths, which were 527nm and 650nm as mentioned by the manufacturer. Further AFM was done in order to find the surface morphology which plays important role in sheet resistance. It was observed that with the coating of QD's roughness of the surface increased.

Electrical measurement was done in order to find the improvement in Current density. As the efficiency of bare Gr/Si heterojunction was observed to be 0.60% which was accurate with literature. After the coating of QD's the enhancement in efficiency was observed which was 1.962%, 1.97%, 2.12% and 2.24% with different samples. Results showed a promising prospect of QD's which can be further used to enhance solar cell efficiency. A significant surge in current density was also observed as compared to literature which was 5.612 mA/cm^2, while our sample showed current density of 7.4 mA/cm^2, 7.57 mA/cm^2, 8.1 mA/cm^2 and 8.2 mA/cm^2. This increase in efficiency is 468% higher then the efficiency reported in literature for Pure Gr/Si Solar Cells.

In future lot of improvements can be done in this type of solar cell. As pristine graphene which was used in our case has high sheet resistance which result in loss of energy can be reduced with the help of chemical doping. With optimization of graphene and using interfacial layer a high efficiency solar cell can be developed which can utilize the QD's emission properties for better PCE.

REFRENCES

[1] Saini, R., Saini, S., & Sharma, S. Journal of cutaneous and aesthetic surgery, (2010). 3(1), 32.

[2] Nasrollahzadeh, M., Sajadi, S. M., Sajjadi, M., & Issaabadi, Z. Interface Science and Technology, (2019). 28, 113-143.

[3] Batra, P. Springer, Cham. (2018). (pp. 81-105).

[4] Pokropivny, V. V., & Skorokhod, V. V.. Materials Science and Engineering: C, (2007) 27(5-8), 990-993.

[5] Battaglia, C., Cuevas, A., & De Wolf, S. Energy & Environmental Science, 9(5), (2016). 1552-1576.

[6] Yoshikawa, K., Kawasaki, H., Yoshida, W., Irie, T., Konishi, K., Nakano, K., ... & Yamamoto, K. Nature energy, 2(5), (2017), 1-8.

[7] Bhopal, M. F., ur Rehman, A., won Lee, D., & Lee, S. H. Journal of the Korean Physical Society, 66(5), (2015). 730-738.

[8] Ghattas, N. I. Middle and High School Science Teachers' Attitudes toward Nanotechnology and Intention to Implement it in Science Classrooms. (2015).

[9] Jean, J., Brown, P. R., Jaffe, R. L., Buonassisi, T., & Bulović, V. Energy & Environmental Science, 8(4), (2015). 1200-1219.

[10] Cui, T., Lv, R., Huang, Z. H., Chen, S., Zhang, Z., Gan, X., ... & Kang, F. Journal of Materials Chemistry A, 1(18), (2013). 5736-5740.

[11] Meyer, E. L., & Van Dyk, E. E. In Sixteenth European Photovoltaic Solar Energy Conference (2020, November). (pp. 2272-2275).

[12] Ko, K. H., Lee, Y. C., & Jung, Y. J. Journal of colloid and interface science, 283(2), (2005). 482-487.

[13] Martin, K. T., de Araújo, O. C., Bonaldo, S. A., & da Silva, M. F. In 2017 Brazilian Power Electronics Conference (COBEP) (2017, November). (pp. 1-6). IEEE.

[14] Lukowski, M. A., Daniel, A. S., Meng, F., Forticaux, A., Li, L., & Jin, S. Journal of the American Chemical Society, 135(28), (2013). 10274-10277.

[15] Mehos, Mark, Craig Turchi, Jennie Jorgenson, Paul Denholm, Clifford Ho, and Kenneth Armijo. Golden, CO: National Renewable Energy Laboratory. 2016. NREL/TP-5500-65688

[16] Wang, X., & Barnett, A. TApplied Sciences, 9(6), (2019). 1227.

[17] Mundada, A. S., Prehoda, E. W., & Pearce, J. M. Renewable energy, 103, (2017). 255-264.

[18] Gerbinet, S., Belboom, S., & Léonard, A. Life Cycle Analysis (LCA) of photovoltaic panels: A review. Renewable and Sustainable Energy Reviews, 38, Life Cycle Analysis (LCA) of photovoltaic panels: A review. 747-753.

[19] Park, N. G. (2015). Materials today, 18(2), 65-72.

[20] Kojima, A., Teshima, K., Shirai, Y., & Miyasaka, T. Journal of the American Chemical Society, 131(17), (2009). 6050-6051.

[21] Li, F., Ji, M., Du, Q., Zheng, J., Jin, M., Shen, Z., ... & Chen, C. The Journal of Physical Chemistry C, 125(14), (2021). 7552-7559.

[22] Kowsar, A., & Farhad, S. F. U. International Journal of Renewable Energy Research (IJRER), 8(3), (2018). 1762-1769.

[23] Roberts, M. W., Clemons, C. B., Wilber, J. P., Young, G. W., Buldum, A., & Quinn, D. D. Journal of Nanotechnology, 2010.

[24] Lee, S. K., Kim, H., & Shim, B. S. Carbon letters, 14(2), (2013). 63-75.

[25] Valenta, J., Juhasz, R., & Linnros, J. Applied physics letters, 80(6), (2002). 1070-1072.

[26] Rasmagin, S. I., & Krasovskii, V. I.. Technical Physics, 66(3), (2021). 476-480.

[27] Chiu, M. H. (2018).

[28] Bhopal, M. F., Lee, D. W., ur Rehman, A., & Lee, S. H. Journal of Materials Chemistry C, 5(41), (2017). 10701-10714.

[29] Li, X., Zhu, H., Wang, K., Cao, A., Wei, J., Li, C., ... & Wu, D. Advanced materials, 22(25), (2010). 2743-2748.

[30] Han, T. H., Lee, Y., Choi, M. R., Woo, S. H., Bae, S. H., Hong, B. H., ... & Lee, T. W. Nature Photonics, 6(2), (2012). 105-110.

[31] Layton, R. A., & Adams, T. M. Introductory MEMS: Fabrication and Applications, 2010.

[32] Reina, A., Jia, X., Ho, J., Nezich, D., Son, H., Bulovic, V., ... & Kong, J. Nano letters, 9(1), (2009). 30-35.

[33] Sutter, P. W., Flege, J. I., & Sutter, E. A.. Nature materials, 7(5), (2008).406-411.

[34] Kim, K. S., Zhao, Y., Jang, H., Lee, S. Y., Kim, J. M., Kim, K. S., ... & Hong, B. H. nature, 457(7230), (2009). 706-710.

[35] Reina, A., Jia, X., Ho, J., Nezich, D., Son, H., Bulovic, V., ... & Kong*, J. Nano letters, 9(8), (2009). 3087-3087.

[36] Somani, P. R., Somani, S. P., & Umeno, M. Chemical Physics Letters, 430(1-3), (2006). 56-59.

[37] Madhuri, K. V. Metal Oxide Powder Technologies, (2020). 209.

[38] Garche, J., Dyer, C. K., Moseley, P. T., Ogumi, Z., Rand, D. A., & Scrosati, B. (Eds.). (2013).

[39] Reina, A., Jia, X., Ho, J., Nezich, D., Son, H., Bulovic, V., ... & Kong, J. Nano letters, 9(1), (2009). 30-35.

[40] Meyer, G., & Amer, N. M. Applied physics letters, 53(24), (1988). 2400-2402.

[41] Gardiner, D. J. Springer, Berlin, Heidelberg. (1989). (pp. 1-12).

[42] Pelant, I., & Valenta, J. Oxford University Press. (2012).

[43] C.B. Honsberg and S.G. Bowden, “Photovoltaics Education 2019.

[44] Kuang, Y., Liu, Y., Ma, Y., Hong, X., Yang, X., & Feng, J. Journal of Nanoelectronics and Optoelectronics, 10(5), (2015). 611-615.